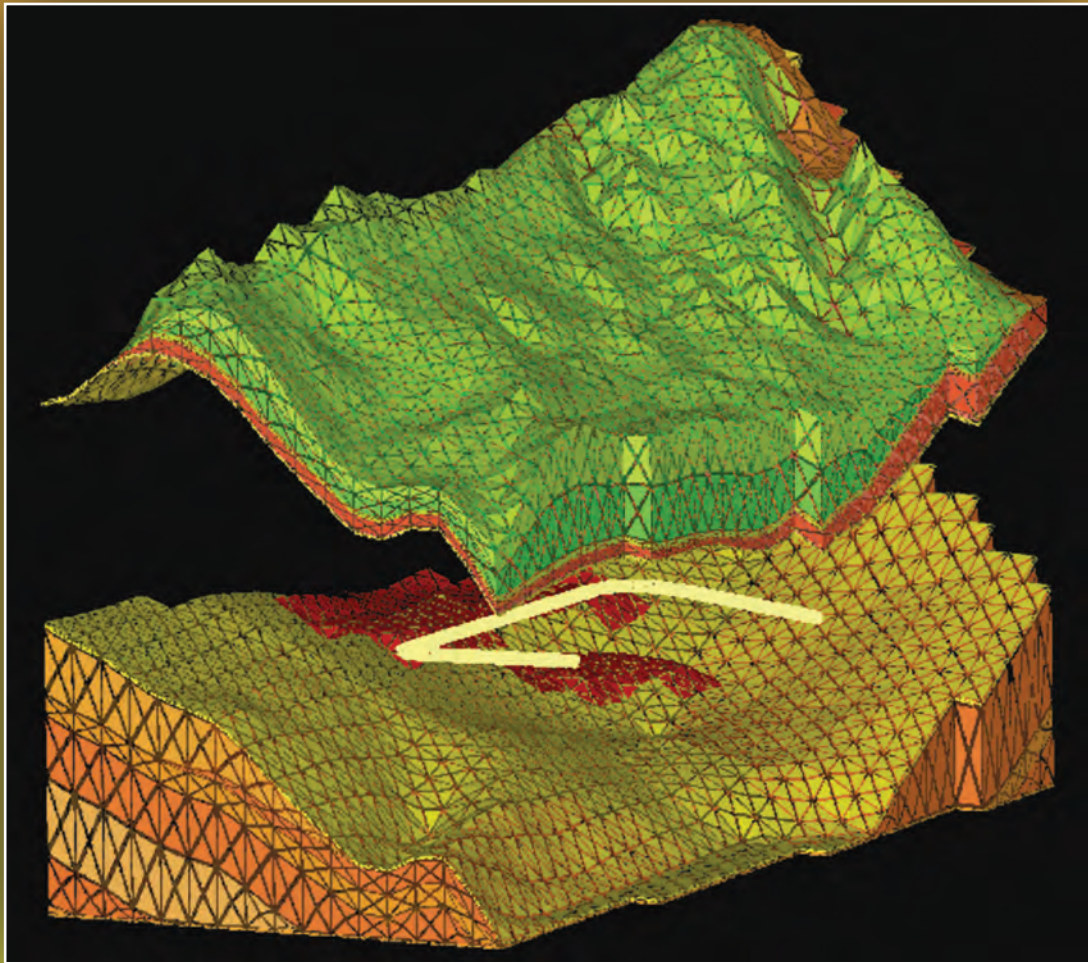


nuclear
weapons
journal



Summer/Fall 2004

- Buried Target Defeat ■ Low-Velocity HE Testing ■
- Uranium Fracture ■ LANSCE Winter School ■ PDMS Polymers ■
- Transmission Electron Microscopy ■ Nonporous Silica Filled Silicones ■



The World's Greatest Science Protecting America

Contents

Point of View	1
Hard and Deeply Buried Target Defeat	2
Low-Velocity Impact Testing of High Explosives	6
Uranium Fracture Experiments and Simulations	10
LANSCE Inaugurates Winter School on Neutron Scattering	13
Transmission Electron Microscopy— a Historical Perspective	16
Mechanical Properties of Nonporous Silica-Filled Silicones	20
Mechanical Properties and Filler Distribution in Silica-Filled PDMS Samples	24
How Atomic Force Microscopy Works	28
The Engineering Institute	30
Developing Structural Damage Prognosis Solutions	32
Water Conservation: Avoiding a Crisis	36
Classified Removable Electronic Media: a Proactive Approach	38
The Intergrated Work Management Process	40
Acronyms	44

About the cover: Detailed computations follow ground-shock propagation to determine how ground shock affects a targeted underground facility. Adaptive mesh development includes creating 3-D models of a target setting and a complex geometric mesh that represents the geologic model.

Summer/Fall 2004 LALP-04-013

Nuclear Weapons Journal highlights ongoing work in the nuclear weapons program at Los Alamos National Laboratory. *NWJ* is an unclassified, quarterly publication funded by the Nuclear Weapons Program Directorate.

Managing Editor-Science Writer
Margaret Burgess

Science Writer-Editors
Larry McFarland
Jan Torline

Designer-Illustrator
Randy Summers

Editorial Advisor
Jonathan Ventura

Technical Advisor
Sieg Shalles

Printing Coordinator
Lupe Archuleta

Send inquiries, comments, and address changes to nwpub@lanl.gov or to Los Alamos National Laboratory Mail Stop F676 Los Alamos, NM 87545



The World's Greatest Science
Protecting America

Los Alamos National Laboratory, an affirmative action/equal opportunity employer, is operated by the University of California for the US Department of Energy under contract W-7405-ENG-36. All company names, logos, and products mentioned herein are trademarks of their respective companies. Reference to any specific company or product is not to be construed as an endorsement of said company or product by the Regents of the University of California, the United States Government, the US Department of Energy, or any of their employees.



Point of View

The Congressional Authorization and Appropriations Process

How does the Laboratory receive funding for its projects and programs? A complex chain of events occurs between the Executive and Legislative Branches before the Laboratory receives any federal money.

Overview

Each year Congress must pass two critical pieces of legislation—an authorization and an appropriations bill—that allow NNSA and its laboratories to carry out the Stockpile Stewardship Program. Unlike other federal agencies, which operate with multiyear authorizations (NASA, for example), the DOE and DoD require an annual authorization bill from the House and Senate Armed Services Committees. The National Defense Authorization bill provides both policy controls and a “funding ceiling” for all DoD activities and DOE nuclear weapons, nonproliferation, and environmental remediation activities.

In addition, 13 appropriations bills—one from each appropriation committee—must be passed by September 30 each year to continue government operations at the start of the new fiscal year on October 1. NNSA and its laboratories are funded by one of these appropriations bills, the Energy and Water Development Appropriations bill. Failure to pass appropriations bills requires Congress to pass a continuing resolution (CR) or shut down government operations for those agencies without an appropriations bill. When federal agencies are working under the terms of a CR, no new starts (e.g., programmatic or construction) are permitted. Funding ceilings are set at the current year’s funding level, or the lower of either the House- or Senate- passed appropriation bill.

Authorization Process

The authorization process begins with submittal of the President’s budget to Congress in late January/early February. The budget is then assigned to

the relevant oversight committees; for NNSA they are the House and Senate Armed Services Committees. Because of the broad scope of oversight responsibilities, each committee is supported by six subcommittees that handle specific aspects of the budget request. For the Nuclear Weapons Program, this detailed oversight function is carried out by the Strategic Forces Subcommittees of the House and Senate Armed Services Committees. Rep. Everet (R-AL) and Rep. Reyes (D-TX) chair the House subcommittee; Sen. Allard (R-CO) and Sen. Nelson (D-FL) chair its Senate counterpart. The chair of each committee and a majority of its members represent the majority party. Each party assigns its members to committees, and each committee distributes its members among its subcommittees.

The Energy Secretary briefs members of Congress and committee staff on the broad financial and policy aspects of the budget request. Linton Brooks, the Under Secretary for Nuclear Security and Administrator of NNSA; Everet Beckner, NNSA’s Deputy Administrator for Defense Programs; and their staffs follow these briefings with comprehensive discussions. After the briefings are complete, the professional staffs of the committees review the budget in detail to prepare members for the hearing cycle, which begins in mid-February and can last through April. Cabinet secretaries testify first, usually before the full committee. The Strategic Forces Subcommittees hold detailed hearings on various aspects of the Stockpile Stewardship Program that involve both departmental and laboratory witnesses. Although the committees prefer to conduct open hearings, they also hold closed hearings to permit classified discussions.

Once the hearings are complete and the Executive Branch provides the follow-up materials (hundreds of pages of questions and answers and inserts for the

continued on page 42

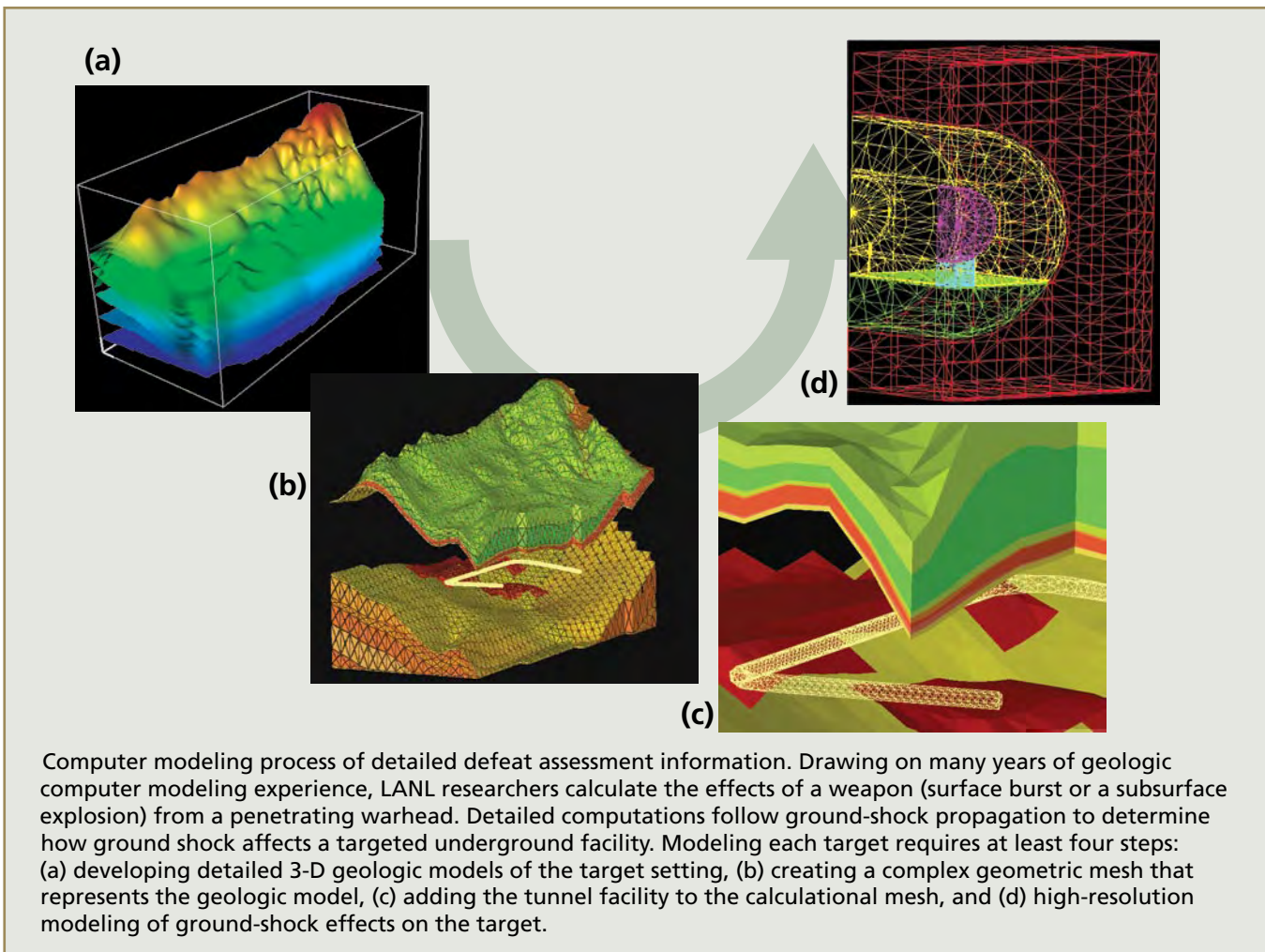
Hard and Deeply Buried Target Defeat

Satellite imagery has improved rapidly over the past few decades, allowing intelligence analysts not only to distinguish an individual vehicle on a road, but also to identify its make, model and, in some cases, its license plate.

In response, governments that want to conceal their activities from prying “eyes in the sky” have increasingly chosen to literally go underground to conduct their most sensitive activities. Underground bunkers, tunnels, and large complexes bolster secrecy; the overlying rocks and earth provide significant protection against enemy attack.

Many of these structures are enigmas because government analysts have not yet determined their layout, purpose, and operational status. This proliferation of underground facilities challenges the United States to develop better methods for locating and characterizing these complexes. We also must develop better predictive capabilities that will help us determine whether an attack strategy, if necessary, would cripple or eliminate such installations.

LANL and the other DOE/NNSA weapons laboratories, in conjunction with DoD and its contractors, are addressing these problems by



- producing accurate 3-D geologic models;
- developing realistic material models for a variety of rock types;
- developing state-of-the-art codes that include hydrodynamics, lithostatic pressures, and rock-damage models; and
- developing more sophisticated facility structural response calculational tools.

Better modeling is needed to improve weapons defeat assessment.

Currently, LANL, LLNL, and SNL/NM are participating in an advanced concepts technology demonstration (ACTD) project on tunnel target defeat. The Defense Threat Reduction Agency (DTRA) administers the project, which is sponsored by the US Strategic Command. The ACTD approach includes verifying and validating computer models of predictive capability by (1) modeling subscale tests as well as an intermediate-scale test in uniformly jointed brittle rock and (2) conducting a full-scale test in a tunnel facility at the Nevada Test Site. LANL applies its expertise in the areas of 3-D geologic characterization, material models, stress-wave propagation codes, structural response models, visualization, and meshing. A computational mesh identifies discrete, representative points on a geometric grid to indicate geologic and/or structural elements in an area of interest, in this case in a potential hard and deeply buried target (HDBT).

In December 1970, LLNL conducted an underground nuclear test that released a large cloud of steam and entrained radioactive gases in the atmosphere. This large and unexpected release was associated with a geologic fault many meters distant from surface ground zero rather than with the test emplacement hole and stemming materials. However, this release was the first real demonstration of the importance of thoroughly understanding geologic influences on underground nuclear explosion phenomena. In response, both LLNL and LANL initiated extensive containment programs

Containment of Radioactivity During Testing: 21 Years of Success

Since 1971, no radioactivity has been released to the accessible environment. From that time to the beginning of the nuclear test moratorium in 1992, LANL conducted 157 underground nuclear tests at the Nevada Test Site. For each test, the Los Alamos containment program provided containment design. Containment design includes

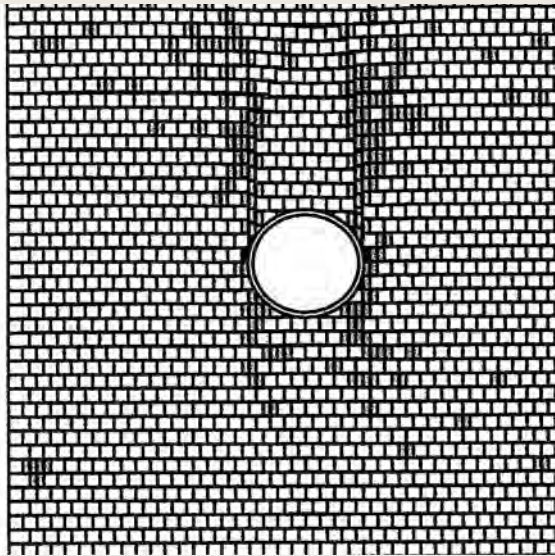
- hole selection,
- depth of burial,
- geologic characterization,
- stemming design, and
- test phenomena prediction.

The containment program currently is centered in the EES Geodynamics Group, a team of scientists from several LANL groups.

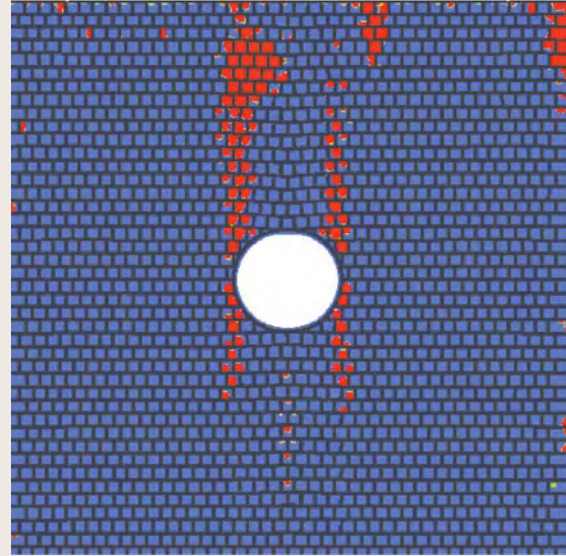
LANL containment activities fall into six major categories:

- hiring and training new personnel to serve as containment scientists, geologists, and modelers;
- updating and enhancing containment databases and database interfaces;
- developing modern 3-D stress-wave codes;
- modifying porous-flow codes to address containment issues;
- identifying and predicting performance of new stemming materials; and
- developing new containment diagnostics sensors and analysis software.

LANL's vital support of these activities ensures that the United States could maintain its ability to contain underground nuclear tests well into the future.



(a)



(b)

DTRA Mighty North test. This test, designed to simulate an explosion in a brittle, jointed rock such as limestone, was instrumented to record exactly where damage occurred and to determine how damage to the surrounding rock deformed the test bed “tunnel.” Researchers then attempted to model the simulation results using various modeling techniques and rock-damage models. This effort showed that finite-element and discrete-element codes are excellent tools for modeling the effects of HDBT tunnel damage on jointed rock. Results also indicate that brittle damage models rather than plastic (ductile) damage models most accurately reproduce actual test results. (a) Dark areas in the observation limestone test bed show brittle cracking but no plastic deformation, confirming that the behavior of hard, jointed rock is dominated by brittle failure, not by plastic deformation. (b) Calculations of brittle cracking damage (shown in red) match test observations in a predicted hard-rock response.

that included geologic characterization, geophysical logging and analysis, downhole diagnostics, and stress-wave modeling.

LANL’s current efforts focus on generating geologic models for sites for which available data may be limited (e.g., overt data collection is not possible for some foreign sites). For some sites, existing data (surface geologic maps, seismic surveys, well log data) may be difficult to obtain or translate, or it may be of questionable quality or limited relevance. However, even with minimal data, experienced geologists can project and interpolate available information using their knowledge of typical structural patterns to develop a detailed, credible model and 3-D rendering of a target of interest.

Weapons-Effects Simulations

HDBT defeat analysis uses computational mechanics to predict and simulate (1) the environment that could be produced by an attack on an underground

facility that is perceived as a threat to the United States and (2) the facility’s response to that environment. A high-fidelity HDBT model incorporates geologic structure, material properties, and facility infrastructure in mathematical models of energy deposition, stress-wave propagation, and material and structural response.

We may conduct environment and response calculations separately for structures that are deeply underground and therefore are subject to ground shock that extends significantly distant from the target. In those instances, we use environment calculations to bound subsequent response calculations.

Usually we calculate the target environment with continuum techniques that follow complex, non-linear constitutive models of material response. We model known geologic layers and faults explicitly because they provide impedance contrasts that influence ground-shock environment.

We also incorporate the effects of geologic joints (fractures that traverse a rock without visible displacement) in environment calculations using rock properties that can be measured in a laboratory. Unfortunately, relating in situ properties to laboratory properties is largely empirical and contributes to prediction uncertainties.

Facility Response

Facility response is significantly influenced by discrete block motion that is initiated by ground-shock interaction with the cavity of a targeted underground facility. Large relative motion introduced by block movement cannot be modeled easily with continuum modeling techniques. Consequently, facility response calculations incorporate either

- continuum codes augmented with contact and joint mechanics algorithms or
- discrete-element modeling techniques specifically designed for modeling the interaction of large assemblies of discrete blocks.

Visible by satellite imagery, random fractures, and material heterogeneities that occur at multiple spatial scales distinguish geologic materials from engineering (i.e., man-made) materials, which show more spatial-scale regularity. Unfortunately, the randomness of natural variability introduces uncertainty in both environment- and facility-response calculations, which in turn introduce uncertainty in damage estimates. Any given simulation provides a single facility response and damage estimate, but with a continuum of possible results.


The rational analysis technique incorporates results from several simulations that are designed to bound environment- and facility-response predictions. The iterative nature of this approach makes advanced simulation and computing (ASC) computer codes and resources ideal environments for achieving required analysis speed and spatial resolution. The tunnel target defeat ACTD provides tunnel response and environment data that permit calibration and sensitivity analysis of HDBT weapons-effects simulations.

RNEP Development at Los Alamos

Robust nuclear earth penetrator (RNEP) development is constrained to competition between a B61 and B83 nuclear explosives package (NEP) contained in a penetrator body. (LANL is tasked with developing the B61 and LLNL is developing the B83.) RNEP is designed to improve future B61-11 (Modification 11 of the B61) capability.

LANL scientists are analyzing and conducting limited hardware tests to assess how to improve the B61's physical capability. Physical differences between the B61 and B83, such as weight, diameter, and internal modifications for "improved robustness," determine penetration ability in different geologies; penetration ability and depth of burial determine how efficiently an NEP couples its energy to the ground and holds at risk or defeats specific HDBTs. Depth of burial and weapon yield also determine collateral effects.

In addition to our current B61 hardware studies, LANL provides critical analytical support to integrated product teams for RNEP phenomena, operational requirements data, planning and cost analysis, and tests of geologic joints.

The current Congressionally mandated study initiated in May 2003. Its projected completion date is late FY06. However, Congressional budget cuts eliminated LANL funding and delayed the New Mexico team's effort by approximately 9 months; the remainder of NNSA's RNEP funding was diverted to the LLNL team until FY05. Fortunately, much of the information we gain from this ACDT study will be applicable to future studies, should they be required. 

Points of contact:

Wendee Brunish, 667-5724, wb@lanl.gov

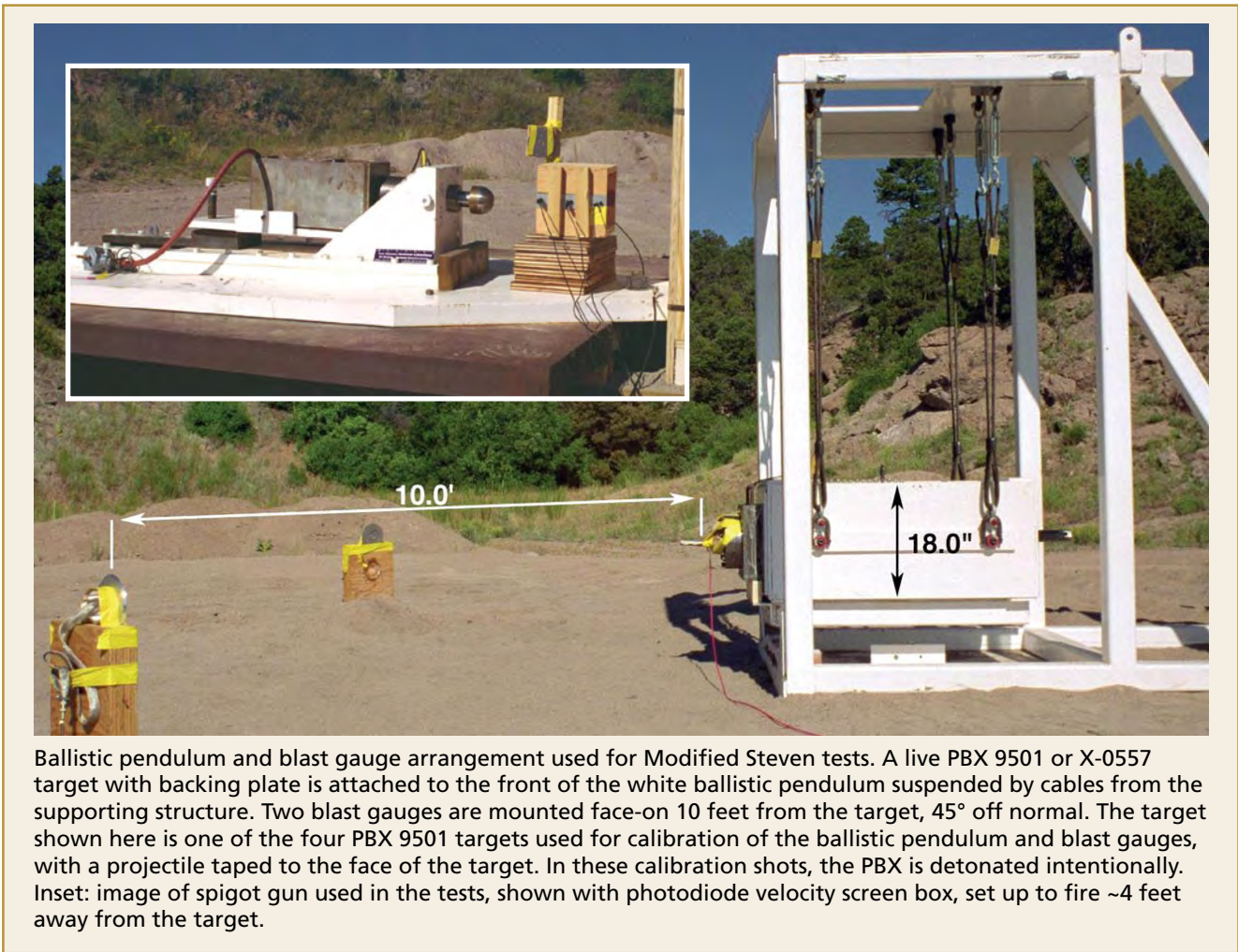
David Steedman, 667-8228, dwsteedman@lanl.gov

Congress eliminated all funding for the RNEP program in the FY05 Consolidated Appropriation Act.

Low-Velocity Impact Testing of High Explosives

The goal of the combined Core and Enhanced Surveillance Programs is to provide experimental data and analyses needed for the physics-based theory and computer models that will improve our understanding of aging mechanisms in the nation's stockpiled nuclear weapons. This improved understanding is crucial to LANL and the broader DOE and DoD communities tasked with addressing tactical and strategic stockpile stewardship demands.

evaluated for potential aging mechanisms that may influence performance or safety. (For more information about the role of Pantex in HE aging studies, see "Monitoring High Explosives Aging—Partnering with Pantex," *Nuclear Weapons Journal*, Winter 2004, pp. 12–15). Ultimately, data derived from these aging analyses will be used to advance predictive capabilities using computer models to assess HE response to mechanical insult.



Ballistic pendulum and blast gauge arrangement used for Modified Steven tests. A live PBX 9501 or X-0557 target with backing plate is attached to the front of the white ballistic pendulum suspended by cables from the supporting structure. Two blast gauges are mounted face-on 10 feet from the target, 45° off normal. The target shown here is one of the four PBX 9501 targets used for calibration of the ballistic pendulum and blast gauges, with a projectile taped to the face of the target. In these calibration shots, the PBX is detonated intentionally. Inset: image of spigot gun used in the tests, shown with photodiode velocity screen box, set up to fire ~4 feet away from the target.

In collaboration with the BWXT Pantex (PX) Plant Surveillance Team, several of the LANL high explosive (HE) formulations used for nuclear weapon components (e.g., PBX 9501) are routinely

The plastic-bonded explosive PBX 9501, a formulation based on HMX HE, has a binder system composed of Estane 5703™ (a polyester polyurethane copolymer), a nitroplasticizer (NP), and small

amounts of stabilizer. One PBX 9501 aging mechanism—NP migration out of the PBX 9501 over time—could potentially lead to increased brittle behavior and response. Changes in the mechanical behavior response of PBX as a function of plasticizer loss eventually may adversely affect how well HE withstands low-amplitude impact—potentially compromising engineering and physics safety requirements.

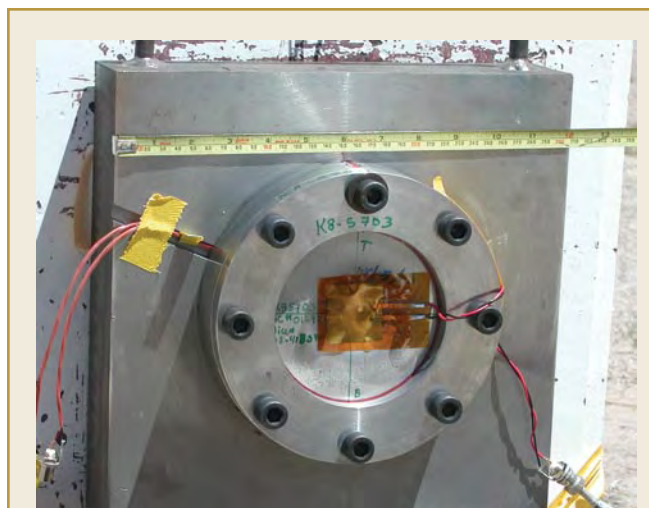
Low-velocity mechanical impact leading to unintentional reaction is of concern in accident scenarios.

Our series of aging tests focused on characterizing the effects of the plasticizer loss on the response of PBX 9501 to low-velocity impacts. That is, we artificially depleted the amount of NP to formulate “virtually aged” lots of PBX 9501 that may mimic one aspect of the aging behavior of PBX 9501.

Low-velocity mechanical impact leading to unintentional reaction is of concern in accident scenarios that involve HE handling, transport, and storage. Various experimental techniques, ranging from small to large scale, have been used to investigate the potential conditions leading to an HE violent reaction (HEVR) for baseline as well as aged HE. The description HEVR can include deflagration behavior and response up to and including detonation.

To investigate the mechanical loading behavior and response of baseline and virtually aged PBX 9501 lots, we used a Modified Steven test geometry consisting of a unique spigot gun design to launch a 2-kg, 3.0-in.-diameter hemispherical projectile ~4 feet at a steel-encased HE target mounted to a ballistic pendulum. Varying amounts of gunpowder, two different barrel designs, and two different types of projectile shanks have been used to achieve projectile velocities ranging from ~20 to ~105 m/s.

The basic target design consisted of a cover plate, holder, and retaining ring. The HE specimens were centered within the target holder and were covered with a 0.020-in.-thick Sylgard 184 layer and the cover plate. The assembled targets were secured to a mild (low-carbon) steel backing plate.



Digital images from quenched, X-0557-1.6 Target K8-5703 showing (top) target intact and attached to backing plate and ballistic pendulum and (lower) evidence of cover plate indentation by projectile impact.

We instrumented our tests with several different types of gauges to measure the projectile velocity, the time of impact, and the back-plate strain behavior of the target. We compared the energy release of the target with calibration data obtained from four baseline PBX 9501 steady-state detonation tests using dynamic (blast overpressure gauges) and static (ballistic pendulum) techniques.

To mimic extreme NP depletion, four lots of X-0557, an HE analogous to PBX 9501, were formulated with reduced NP concentrations for comparison to baseline PBX 9501. The first two lots, X-0557-0.69 and X-0557-0.98, were formulated at LANL. The other two lots, X-0557-1.6 and

X-0557-2.0, were formulated at PX. Specimens were pressed hydrostatically and machined to diameters of 5.0 in. and thicknesses of 0.5 in.

For these tests, our objective was to evaluate and compare the trends in the projectile threshold velocity for the four different X-0557 lots as a function of NP weight percent relative to the baseline PBX 9501 formulation. For the purposes of this discussion, threshold velocity is defined as the minimum velocity range required to achieve an HEVR at least 50% of the time.

We tested a total of 23 samples of X-0557. In the quenched tests, the projectile impact indented the target cover plate, but the target remained intact and usually remained attached to the backing plate. In these tests, “quenched” means that we have seen evidence that a reaction may have been initiated, but was mitigated prior to blowing the target apart. The HEVR behavior in the X-0557 targets ranged from target damage comparable to that of the baseline PBX 9501 tests, with small amounts of HE scattered on the firing mound, to physical damage and energy release that exceeded the baseline PBX 9501 results. The HEVR energy release varied according to impact velocity and NP weight percent.

We also compared HEVR velocity threshold behaviors for the X-0557 targets with data obtained on a baseline PBX 9501 lot (threshold ~ 55 m/s), where 100% energy release represents an intentional detonation of PBX 9501 targets of the same dimensions. These data show the same sharp consistency that we have seen with previous Modified Steven test series with no evidence of mixed-zone (crossover)



Digital images from post-test X-0557-2.0 Target K8-5724 after HEVR showing (top to bottom) target holder, retaining ring, and cover plate damage. In some tests, the target damage was comparable to PBX 9501 baseline tests; in others, physical damage and energy release exceeded baseline results.

results—i.e., no HEVR at lower velocities than the threshold, or quenched events at velocities that exceed the threshold. We have seen evidence in other types of low-velocity impact tests where a target reacts violently at a lower velocity than anticipated from previous results.

A review of the data shows

- a trend toward increasing threshold values with increased NP content;
- two ranges of projectile threshold velocity overlap for the X-0557 threshold data—i.e., the thresholds for the X-0557-0.69 and X-0557-0.98 lots are essentially the same, and the threshold velocities for the X-0557-1.6 and X-0557-2.0 lots are similar; and
- an increase in average energy release as NP weight percent drops.

The overlap in threshold response between the two sets of X-0557 data suggests that significant differences in the plasticizer content are necessary to achieve discernible differences between threshold responses with the Modified Steven tests from baseline PBX 9501.

The data also show that all four X-0557 thresholds are lower than

the PBX 9501 threshold ranges for this target and impactor test configuration. We believe that the reductions in threshold velocity ranges are due to at least two factors that result in changes to the mechanical property response of the HE to low-velocity impact:

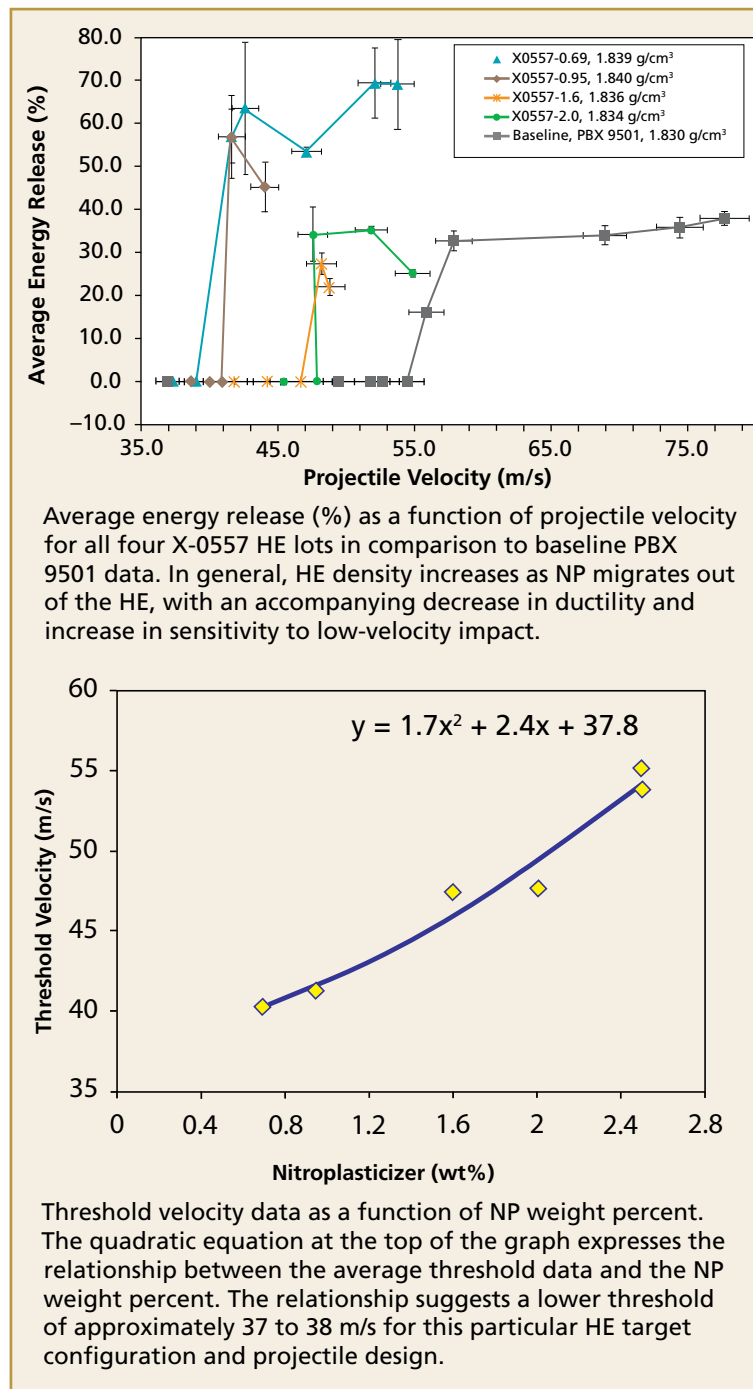
- the effects of reduced plasticizer coupled with increased fractions of HMX and Estane and
- the higher density of the X-0557 targets relative to PBX 9501.

The effects of increased density on low-velocity mechanical loading test results were evident in previous PBX 9501 Modified Steven tests and were further evaluated with lab-scale target testing. Prior PBX 9501 Modified Steven tests showed a threshold velocity decrease of ~ 0.27 m/s per 1 mg/cm^3 density increase in this particular target configuration.

Lab-scale testing demonstrated that the higher-density PBX 9501 targets showed a higher shear strain component than did lower-density targets.

If the shear strain component is a key factor in the ignition mechanism, then a higher shear strain component would result in a reduced threshold range for the higher-density specimens.

Neglecting the density changes and the slight variations in HMX and Estane content, and considering only the change in NP weight percent as the most significant difference, we can derive a simple quadratic relationship ($y = 1.7x^2 + 2.4x + 37.8$) between the average threshold data and the NP



weight percent. This relationship suggests a lower threshold of ~ 37 to 38 m/s for this particular target configuration and projectile design with ~ 95 wt% HMX and ~ 5 wt% Estane formulations.

The X-0557 test results have shown

- an energy release that was never equivalent to a complete detonation of the PBX 9501 but increased with significant NP depletion and
- a remarkably sharp threshold to reaction, lower than for baseline PBX 9501, without evidence of mixed-zone results (crossovers).

Both of these X-0557 test results are believed to be due to differences in composition and density, resulting

in changes in the mechanical response of the HE to low-velocity impact. Further work is required to determine a semiquantitative relationship for threshold behavior as a function of the different variables. [NWJ](#)

Points of contact:

Deanne J. Idar, 667-7695, djidar@lanl.gov

Joseph T. Mang, 665-6856, jtmang@lanl.gov

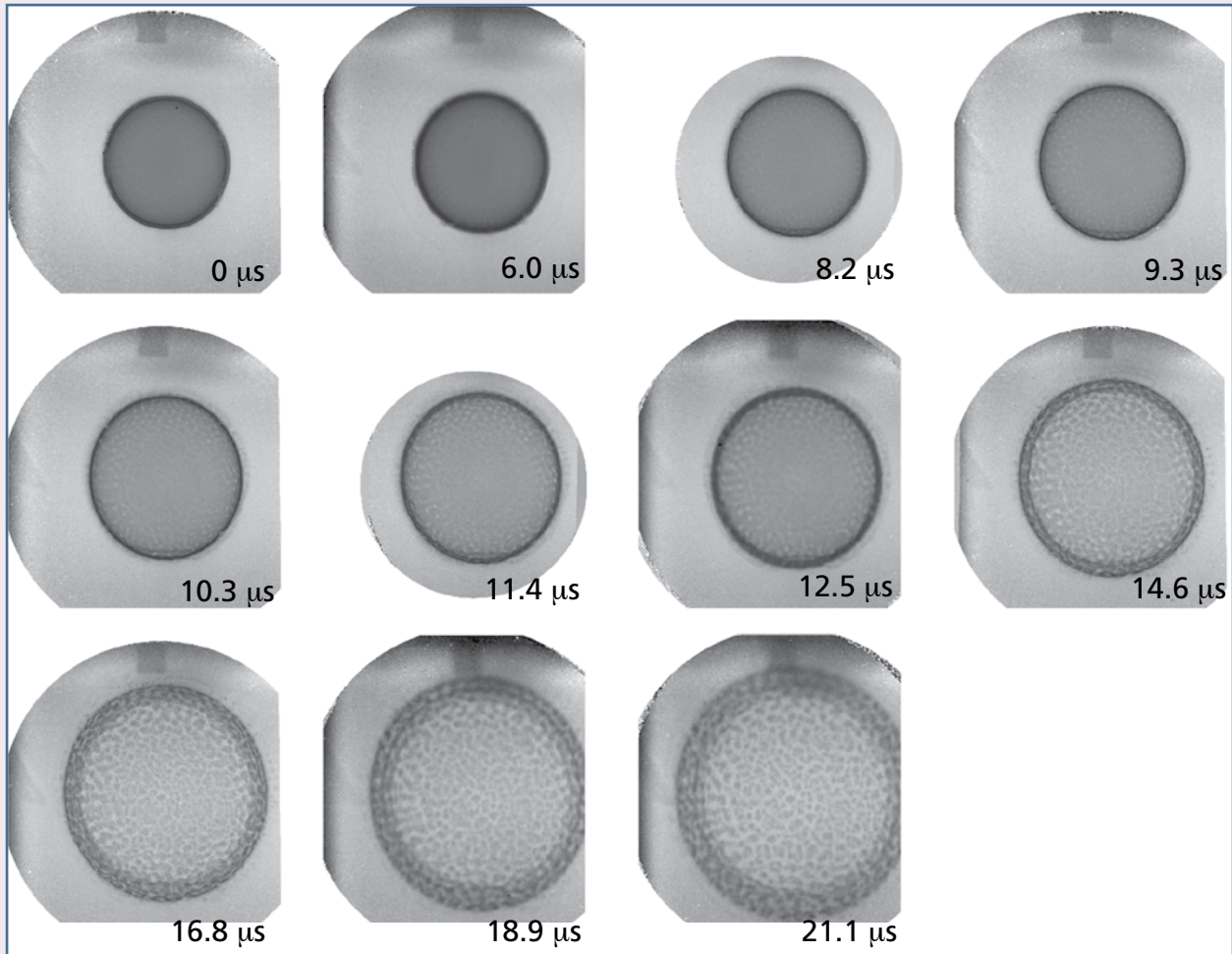
Uranium Fracture Experiments and Simulations

Understanding fracture, also called “failure” or “cracking,” in the materials in the nation’s nuclear stockpile is essential to the Laboratory’s mission of stockpile stewardship. Tasked with determining how materials such as uranium fracture at high strain rates, a team of Los Alamos researchers

from groups CCS-3, X-3, P-25, DX-3, X-4, and T-3 are using proton radiography (pRad) to track the evolution of fracture in depleted uranium (DU).

Depleted Uranium Fracture

Using pRad, these researchers took a radiographic



Proton radiography time sequence images of DU shell fracture. Researchers study time-sequenced images of an explosive-filled DU hemisshell to better understand the dynamics of fracture. The uranium shows a “corn-flake” cracking pattern.

movie of a DU fracture event. In the experiment, they detonated a hemisphere of high explosive (HE) that had a thin outside shell of DU. Analyzing a pRad image time sequence, they traced the evolution of DU's thinning and fracturing into corn-flake-shaped pieces. The size of these "flakes" and the amount of material between them varies, based on the initial thickness of the material and how it was fabricated.

Experimental pRad images reveal the evolution of uranium thinning and fracturing in high-strain-rate conditions.

In the ongoing study, the team measures the density of the flakes and of the dust and other material between the flakes and how these factors evolve over time. The study examined more than 20 experimental pRad images, from detonation ($t = 0$) to approximately 25 μm after detonation, with approximately 200- μm spatial resolution.

Shear-Banding

The onset of shear-banding (localized deformation in the form of thin planar bands that is caused by material softening) is not visible at this spatial resolution. However, these time-sequenced images clearly show fracture evolution, allowing researchers to trace a fracture back to its original failure time. These experimental images can be compared with 3-D calculations that predict regions of high strain.

Using vector algorithms and other image-processing techniques to extract information from the radiographs, the team determine failure onset,

material density in the cracks, and size distribution of the flakes. Then they enter that information into computer-simulated fracture models. In the absence of nuclear testing, scientists use these models to predict fracture onset in nuclear materials and to simulate the materials' failure under high-strain-rate conditions.

Focusing on how materials such as uranium fail by shear-banding, the research team hopes to answer four primary questions about the shear-banding process.

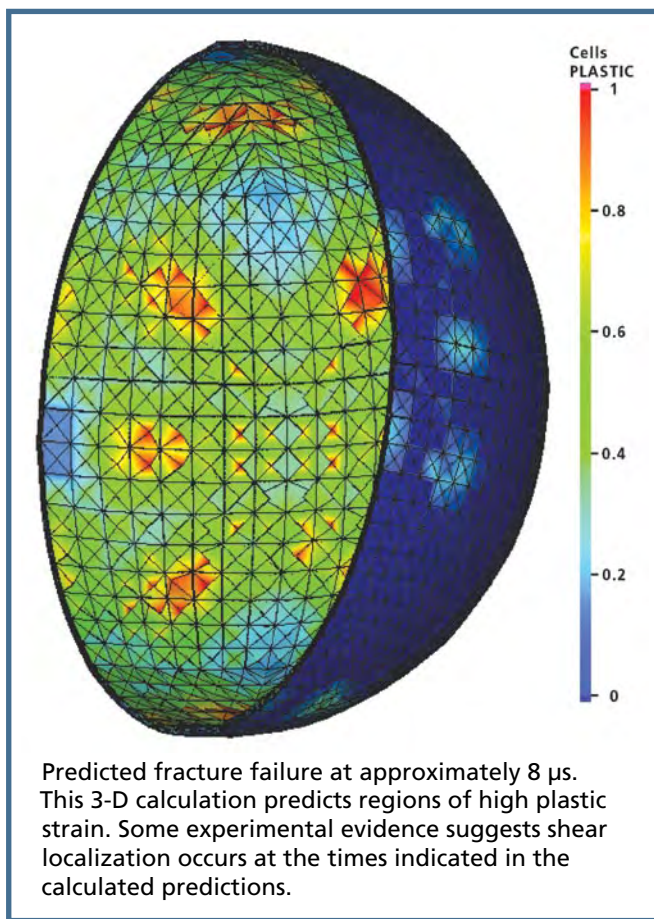
- When does a material start to fail?
- How big are the resulting pieces?
- Does piece distribution vary with spatial location?
- Do the cracks between the flakes contain any material?

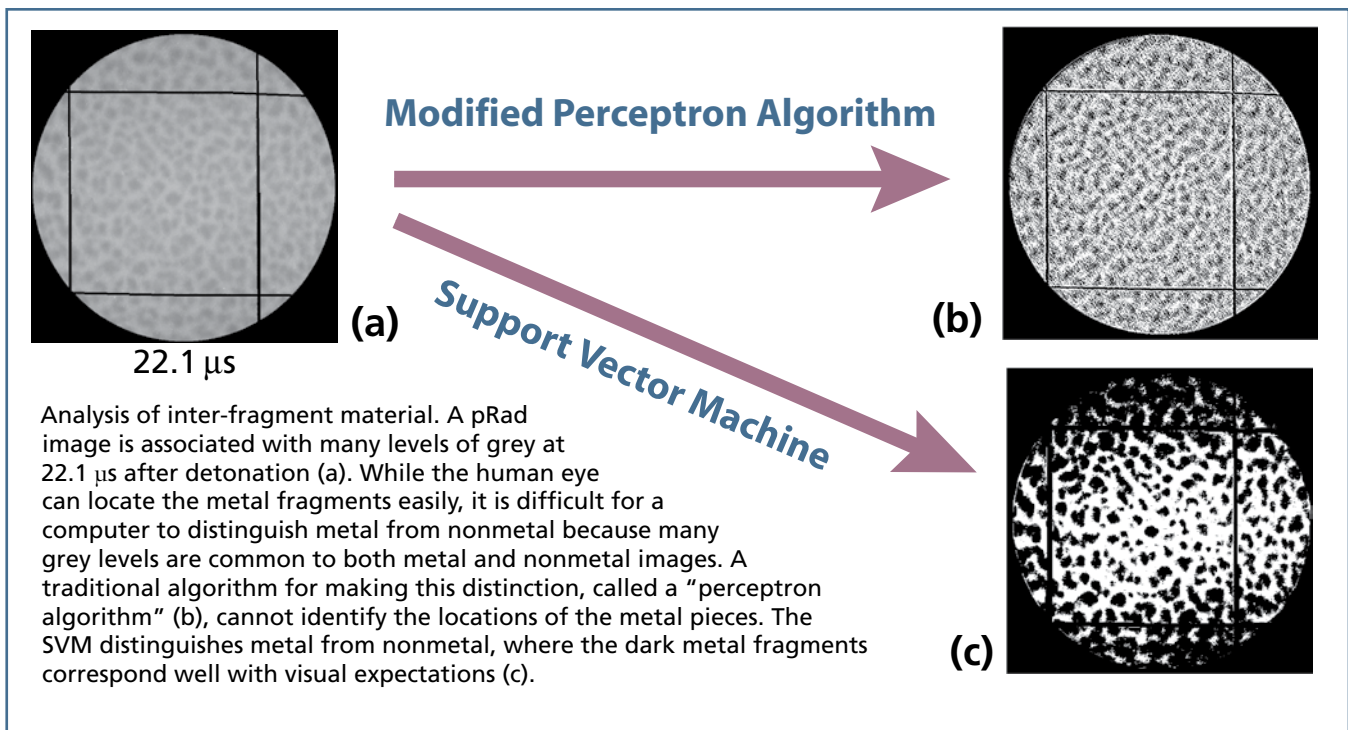
An excellent tool for obtaining this information, pRad's extraordinarily high temporal resolution

pinpoints crack initiation; pRad's spatial resolution captures images of both the fragments and the material, if any, that is in the cracks between the flakes.

Calibration and Density

To calibrate the images and determine the density of the explosive products behind the fracturing hemispherical shell, the team configured experimental steel shots exactly as they had configured the DU shots. Although they achieved 3-D calculations of the uranium experiments, they have not yet achieved material failure in computer simulation.





To date, they can predict only where the material might fail by identifying regions of high plastic strain; calibrating fracture models with quantitative information from the experiments may overcome this limitation. However, the predicted fracture, at approximately 8 μs after detonation of this experimental configuration, is consistent with radiographic data.

The team also investigated HE areal density in the steel shots because steel fractures cleanly, i.e., it leaves very little material in the cracks. This information provided baseline densities for the expanding HE over time; the team then used these baseline densities to examine the uranium shots.

Assuming that the same HE products reside behind the uranium shell, the team determined minimum density values for the material in the cracks. In contrast, they determined maximum density of the material in the cracks by assuming the extreme condition that no HE resided behind the uranium. This assumption put density bounds on the material in the cracks of the expanding, fracturing uranium. Determination of the density of the material in the cracks of a dynamically fracturing piece of DU has never been done before experimentally.

Current analysis focuses on quantitatively determining the locations of metal and open areas (space between the cracks) in the DU shots. Giving 15 colleagues 100 different random points on each image, the team asked them to identify whether each point was on metal or nonmetal. These 1500 data points were used to focus a support vector machine (SVM). The SVM creates a functional description of metal and nonmetal, based upon the 1500 data points. When the SVM encounters a new uncategorized data point on an image, it recognizes whether the material at that point is metal or nonmetal. After scanning all data points on an image, the SVM locates the metal areas (dark regions) on the image, further enabling the team’s ability to investigate material between the corn-flake-shaped cracks. [NWJ](#)

Point of contact:

Katherine Prestridge, 667-8861, kpp@lanl.gov

The research team for this project also included Michael Cannon, Lawrence Hull, Don Hush, Frank Merrill, Mark Potocki, Cynthia Swartz, and Qinhai K. Zuo.

LANSCCE Inaugurates Winter School on Neutron Scattering

The Los Alamos Neutron Science Center (LANSCCE) Neutron Scattering Winter School, inaugurated in January 2004, received an enthusiastic reception from the 30 students who were selected to attend. The school will now be an annual January event, helping to build the community of future neutron scientists for the nation. Each school focuses on a specific topic: magnetism was the 2004 topic, and scattering applications for structural materials will be the topic of the 2005 school. Topics being considered for future years include soft materials, biological applications, and materials at elevated pressure and temperature.

Neutron scattering is a technique used to probe the microscopic structure and dynamics of condensed matter, and it is one of the truly unique and most powerful investigative tools available for the study of both solid and liquid materials. The neutron is an uncharged nuclear particle, and thus neutrons fully penetrate most materials. Neutron scattering provides true three-dimensional information on the microscopic structure of materials on length scales ranging from interatomic dimensions (a fraction of a nanometer) up to micrometer sizes. In addition, because the neutron carries a magnetic moment, the scattering also contains information about magnetic properties of the material. Furthermore, the energy of a thermal neutron is in the range of most elementary excitations in solids such as phonons (lattice vibrational waves) and magnons (the wave character of magnetism). Neutrons have the ability to create and annihilate such excitations (inelastic scattering) and thus provide detailed information on the characteristics of the phonons or magnons.

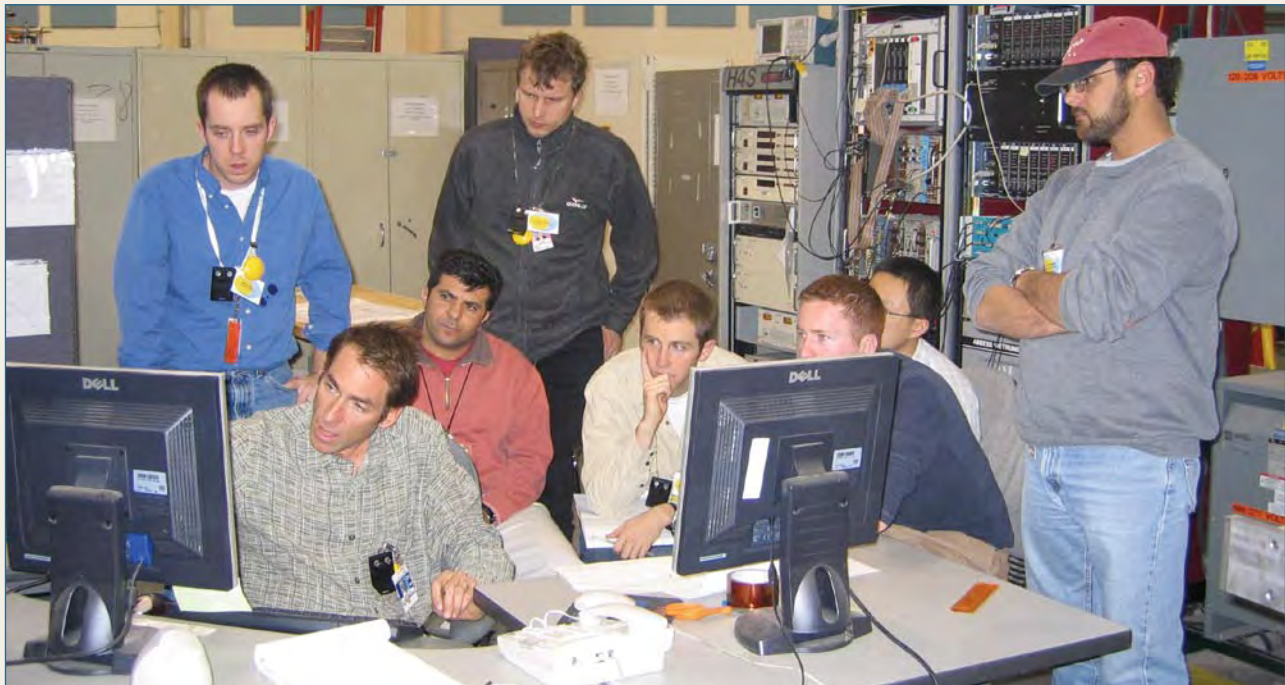
Los Alamos has one of the most powerful neutron scattering facilities in the world, with a highly ver-

satile instrument suite available for materials studies. The Manuel Lujan Jr. Neutron Scattering Center at LANSCCE operates 11 scattering instrument beam lines that derive neutrons by the spallation process from a tungsten target. The proton beam striking a surface on the spallation target has a typical current of 130 μA , provided by the LANSCCE 800-MeV accelerator at a repetition rate of 20 Hz. A series of very creatively designed low- and room-temperature neutron moderators tailor the spallation energy spectrum for the scattering instruments. The LANSCCE facility will retain its dominant position as the most intense pulsed neutron source in the US until the Spallation Neutron Source, currently under construction at Oak Ridge, begins operating in 2006.

Neutron scattering has wide application to research problems in condensed matter physics, materials science (including polymers, composites, and porous materials), biological systems, geomaterials, and engineering materials. Examples of many of these types of problems and the relevant facilities available at the Lujan Center can be found in the 2003 review article in this journal. (See May/June 2003, "The Lujan Center and Neutron Scattering," pp. 16–21.) At the Lujan Center, a significant fraction of the research is devoted to national security problems, including nuclear weapons materials research. Some recent examples include the determination of the phonon density of plutonium, accelerated aging reactions in uranium-niobium alloys, investigation of erbium deuteride and tritide systems, and investigation of energy levels and possible magnetism in plutonium.

Scattering Research and Outreach

Historically, neutron scattering facilities have been



One of three groups of students from the LANSCE Winter School on Neutron Scattering performing a “hands-on” experiment.

the domain of the national laboratories because they require large neutron sources (reactors or accelerators). Surprisingly, the unique benefits of neutron scattering techniques for materials research are still not well understood and are underappreciated in the US academic community. Over about the past 15 years, the DOE’s national laboratories and the National Institute of Standards and Technology (NIST) have instituted national user programs intended to open the neutron facilities to the wider external research community. Time on scattering instruments is open to users both outside and within the laboratories, with allocations based on a proposal system and peer review by program advisory committees. This availability has resulted in a significant increase in the number of users visiting the national laboratory neutron scattering facilities. The accompanying graph shows the dramatic growth in number of users at the Lujan Center over the last few years, approaching 600 during the 2003–2004 run cycle.

Additional efforts have been made to broaden the awareness and significance of neutron scattering in the national research community, particularly among graduate students and postdoctoral researchers, by instituting short neutron schools at three

major facilities. One- or two-week summer schools were begun in the 1990s at Argonne National Laboratory and at the NIST Center for Neutron Scattering. The Argonne school is at an introductory level and includes both neutron and x-ray (synchrotron radiation) scattering. The NIST school concentrates on neutron scattering applications on specific instruments.

The LANSCE school is unique because it is the only school that provides an in-depth educational experience on a specific research topic that is impacted in a major way by neutron scattering. The LANSCE school attracts graduates from the other two neutron schools who are interested in pursuing a specific area of research. The topical focus of the LANSCE school will change each year on a 4- or 5-year cycle corresponding with the approximate transit time for students in graduate programs.

The 2004 LANSCE Neutron Scattering Winter School was advertised to the external education community via posters and a web site. Applications were invited from advanced undergraduate students, graduate students, and postdoctoral researchers. The intent was to limit the number of students to 20. However, 54 applications were received, a strong

testament to the external demand for outreach opportunities in this field. Because of the intense demand, enrollment was expanded to 30 students, who came from 15 states and one foreign country.

The students were given the opportunity to spend 7 days at Los Alamos listening to lectures and performing “hands-on” experiments using four of the Lujan Center spectrometers. The students could select from three

experiments to be performed during the week that were planned to acquaint students with sample preparation, experiment planning, setup of the instruments, and data analysis.

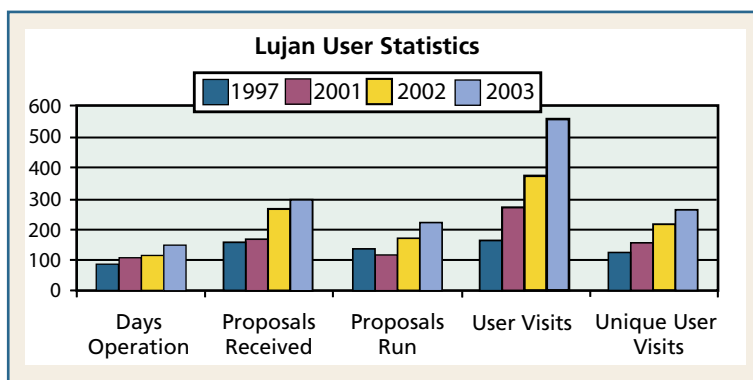
Students had the opportunity to

determine the magnetic and crystal structure of a perovskite manganite material with the high-intensity powder diffractometer, examine magnon dispersion in a rare earth crystal using Pharos (the inelastic scattering spectrometer), look at thin magnetic multilayers on Asterix (the polarized beam reflectometer), and study magnetic critical scattering on the low-Q diffractometer. Many of the students chose experiments closely related to their thesis topics, while others used the experience to broaden their general knowledge of the impact neutrons could make on understanding magnetic systems. Each group of students was required to give a presentation on the results of their experiment on the last day of the school.

The lecture portion of the school consisted of 16 lectures given by 14 world-renowned experts in the field of magnetism and neutron scattering on topics such as thin-film magnetism, spin waves, and crystal-field excitations. Talks covered the theory of magnetism and magnetic neutron scattering as well as experimental investigations of magnetic systems via neutrons, x-rays, and conventional techniques. The students and lecturers were given ample opportunity to interact and ask questions in the school’s informal environment.

At the end of the weeklong school, students were asked to evaluate the lecturers, scattering laboratory experiments, and other aspects of the school program and organization. These evaluations were numerical and also contained detailed written comments. We, the advisory committee for the school and the LANL scientists involved, were extremely pleased with the overall high level of satisfaction with the lecture program and organization aspects

of the school. The most common criticism was that not enough time was allocated to the experiments and to the data analysis, and the students recommended extending the school to 9 days to accommodate more experimental time.



The Lujan Center looks forward to hosting many more successful neutron schools in the coming years, and to making significant contributions to the future development of this field for the benefit of Los Alamos and the nation. [NWJ](#)

Point of contact:

James J. Rhyne, 665-0071, rhyne@lanl.gov

During the 2002 run cycle at the Lujan Center, the newly commissioned 11-T super-conducting magnet provided users with the first results of an intensity image (reflection) of neutron data collected from an antiferromagnetic material on the new Asterix instrument.



Transmission Electron Microscopy— A Historical Perspective

Although LANL research scientists knew for many years that high voltage enhances specimen penetration, the nature of the factors that limit the maximum usable specimen thickness for different materials was not clearly understood. Researchers did know, however, that the value of specimen thickness limit decreases for materials with larger atomic numbers, including plutonium.

Developing techniques to obtain the extremely thin foils needed to examine such an easily oxidized, highly toxic compound was difficult. As early as the 1960s, however, LANL researchers conducted some of the first transmission electron microscopy (TEM) investigations to enhance image contrast of metallic plutonium and plutonium alloys. Although it was abandoned by 1967 due to technical constraints, this early work identified three fundamental issues associated with plutonium thin-foil preparation:

- specimen oxidation,
- electron transparency at 100 kV, and
- low thermal conductivity.

LANL researchers originally concentrated on producing films created directly by vapor deposition and splat cooling, but the investigation quickly switched to thin foils of bulk material (plutonium). The mechanical behaviors of delta-stabilized plutonium and aluminum are similar; delta-stabilized plutonium has a large temperature/composition stability range.

Delta-phase plutonium (alloyed with aluminum or gallium) became the material of choice. First, it could be cold-rolled and fabricated into 5-mil-thick sheets that were suitable for electrochemical thinning. Second, delta-phase plutonium was more representative of the bulk material that reflected the microstructure in the samples. Third, high-purity,

electrorefined alpha plutonium was available for alloying.

Specimen Oxidation

These early LANL efforts produced foils with heavy surface layers of oxide on which only the boundaries of the metal grains could be discerned with confidence. Unfortunately, the foils deteriorated in the microscope. Electron-beam heating of these foils caused the metal to react with residual oxygen in the microscope, rapidly transforming the plutonium foil into films of well-defined grains of plutonium oxide. Also, the window technique, commonly used at that time to produce TEM foils, generated excessive amounts of contaminated electrolytes and rinse solutions. Each foil required many hours of preparation that rarely produced viewable foils.

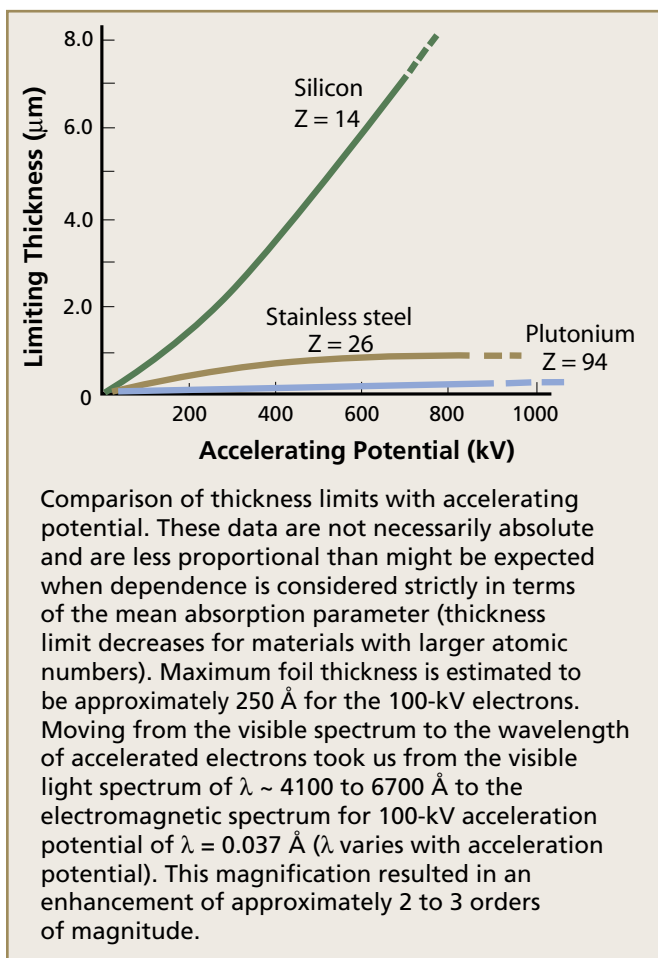
Electron Transparency

Unfortunately, most 1960s sample preparation attempts did not include the use of bulk plutonium, without which representative microstructures could not be obtained. Those experiments all required reducing sample thickness mechanically by rolling, which deformed the microstructure, or cutting slowly with a diamond blade to minimize heat generated by the cutting process. The samples were thinned even further by sanding/lapping to a thickness of approximately 1 to 2 mil and then electropolishing or ion thinning them to electron-transparent thickness of approximately 250 Å.

Ion thinning yielded no usable foils, however, because the ion guns of the early 1960s did not have sufficient intensity and beam focus, or extremely low metal-removal rates. Also, the foil surfaces were rough and had no uniformly thinned regions.

Low Thermal Conductivity

Already working with extremely thin foils (approximately 250 Å for 100-kV electrons), LANL



scientists correctly expected the thinning process to become increasingly difficult as the foils became even thinner. In addition to plutonium’s characteristically strong oxidation properties, its low thermal conductivity implied that energy input from the electron beam would heat the sample temperature during observation in the microscope. This temperature rise increased the already high oxidation rate and also could have induced phase transformations.

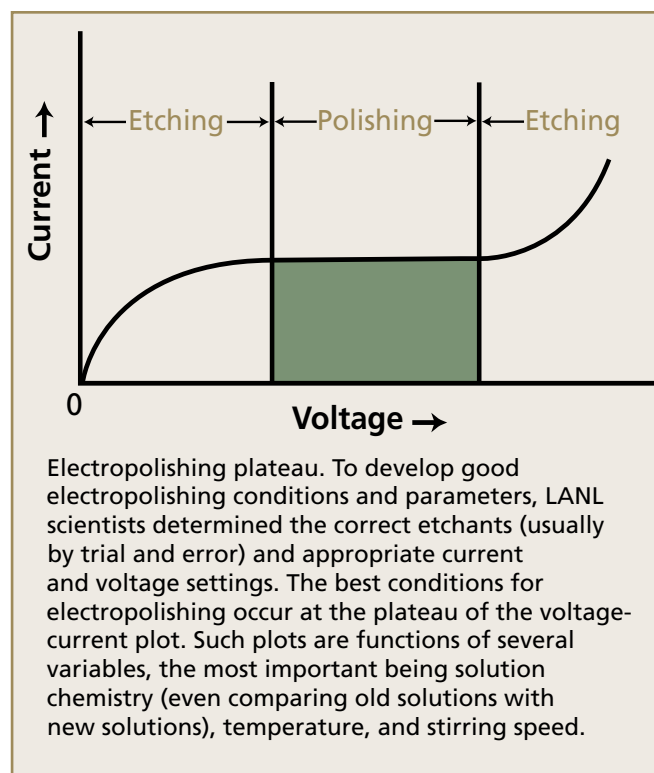
Specimen Preparation

The earliest reported attempts to prepare electron-transparent foils generally followed two approaches: evaporation and splat cooling. Although all attempts to prepare evaporated thin films produced foils of plutonium oxide, splat cooling produced the thinnest foils.

Splat-cooled molten plutonium samples were quenched from the molten state. A shock pulse ejected a small bead of molten metal through a 1-mm-diameter hole in the bottom of a ceramic crucible onto an inclined, relatively massive, water-

cooled copper target plate. These rapidly quenched samples were porous and consisted of many “thin” overlapping foils of irregular size and shape that sometimes stuck together.

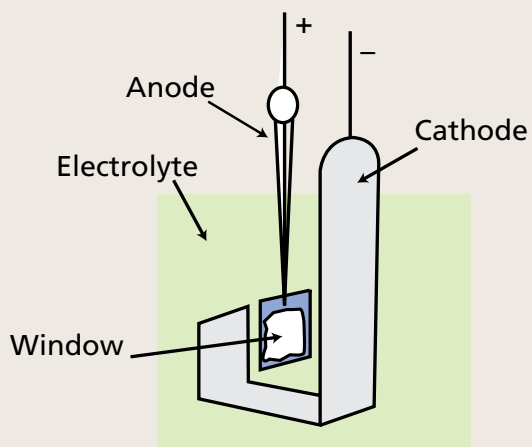
Individual foils varied in thickness from a few hundred angstroms near the edges to many micrometers at the centers. Unfortunately, the samples showed heavy oxide deposits in regions thin enough for electron transparency, which prevented accurate observation of the microstructure of the metal alloy. Beam heating quickly converted the remaining metal to plutonium oxide.



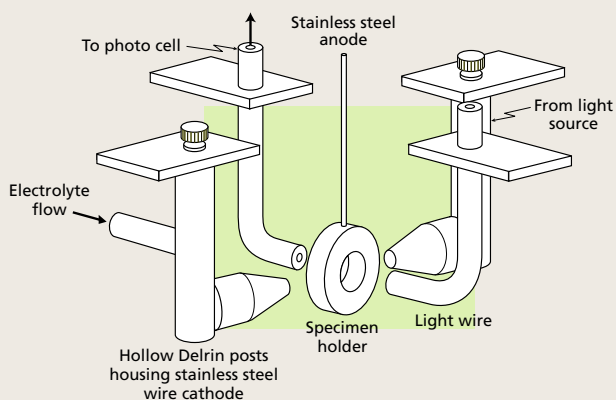
Most of these attempts produced only oxide thin films. Scientists at other research centers also experimented with “coating” the thin foils with a low-atomic-mass element (such as beryllium, carbon, and magnesium) to “protect” the metallic plutonium. They attempted this technique for splat-cooled, ion-thinned, and electropolished samples to protect them during handling and to minimize beam heating in the electron microscope. Unfortunately, coating also failed to prevent further oxidation.

Advances in the 1980s

In 1981, renewed programmatic interest at LANL focused on finding an electropolishing solution, using



Window technique. Commonly used during the early years of electron microscopy, this method of specimen preparation enables selective electrolytic removal (thinning) of a flat sample that has been painted at its edges with a protective lacquer. The specimen is suspended in the electrolytic cell; properly adjusted current and voltage create holes in the window of the foil; electron-transparent portions then can be extracted for examination.



Polishing arrangement. In the 1960s, LANL researchers used a more sophisticated polishing technique that included an automatic cutoff for the polishing current. A motor drove a pump that forced the electrolyte through a hollow, movable post that housed cathodes. The wires were enclosed in glass tubing, which was submerged in the polishing solution. Light transmitted from an outside source struck one side of the specimen; when the specimen perforated, the transmitted light struck the opposite side of the specimen. That light, transmitted to an outside photocell, energized a solenoid that shut off the polishing current and sounded an alarm. Technicians removed the specimen holder, rinsed it first in acetic acid and then in methyl alcohol, removed the disk from the holder, and rinsed it in alcohol. The noise of the alarm alerted technicians to remove the specimen, thereby minimizing contamination that occurred if the specimen was left in solution after polishing was completed.

a newer, commercially available jet-type thinner. The jet thinner focused the electrolyte onto a small portion of sample that was being thinned, which increased control of the electropolishing current.

An appropriate electropolishing solution was found by working with solutions that had been used successfully to prepare thin foils of stainless steels and ferritic steels. The best plutonium foils were produced when the electrolytic solution (seven parts acetic acid and one part perchloric acid) was cooled from 10°C to 13°C and operated at 15 V. To further diminish oxidation during electropolishing, the research team bubbled argon through the solution for several hours to ensure oxygen displacement. Immediately after perforation, the researchers washed the foils in cold ethyl alcohol to remove any traces of the electropolishing solution.

Better control of the sample preparation environment eliminated oxidation. First, all operations were conducted in a glovebox. Second, the team designed and built a highly successful transfer unit for the sample holding device that facilitated inserting the foil into the microscope without exposing the thin foil to air. This process ensured that prepared foils could be safely withdrawn from the glovebox, moved into the transfer unit, and finally inserted into the electron microscope without exposing the thin foil to air at any time. This breakthrough technique, crucial to TEM examination of plutonium thin foils, also minimized potential contamination issues.

Several other factors contributed to achieving usable images and confirmatory data on metallic plutonium:

- newer and better twin-jet electropolishers, with more precise optical current cutoffs, that created thin foils at the moment of foil perforation;
- microscopes with much better vacuum, resolution, and diffraction capabilities and twice the accelerating voltage than those of the 1960s;
- advances in plutonium metallography;

- improved inert-gas quality and inert-system capabilities;
- significant changes in TEM capability and TEM column vacuum technology; and
- advanced diffraction-analysis computer techniques.

These capabilities, considered “advanced” by 1980s standards, combined with a glove-box environment and the new unique transfer device, resulted in greater penetration of slightly thicker foils.


TEM Then and Now

TEM has produced a wealth of otherwise unobtainable information since its first reported application almost 60 years ago. In the early 1960s, preliminary results on plutonium 1 wt % gallium thinned by electropolishing were not successful. However, scientists involved in TEM research at that time thought these experiments involved the oxide rather than the metal. TEM showed that certain crystal orientations of delta-stabilized plutonium oxidize epitaxially; i.e., the metal and its oxide have the same crystal orientation. Furthermore, diffraction spacing for both crystals, clearly visible on 21st-century electron microscopes, was not discernable with then-current microscopes.

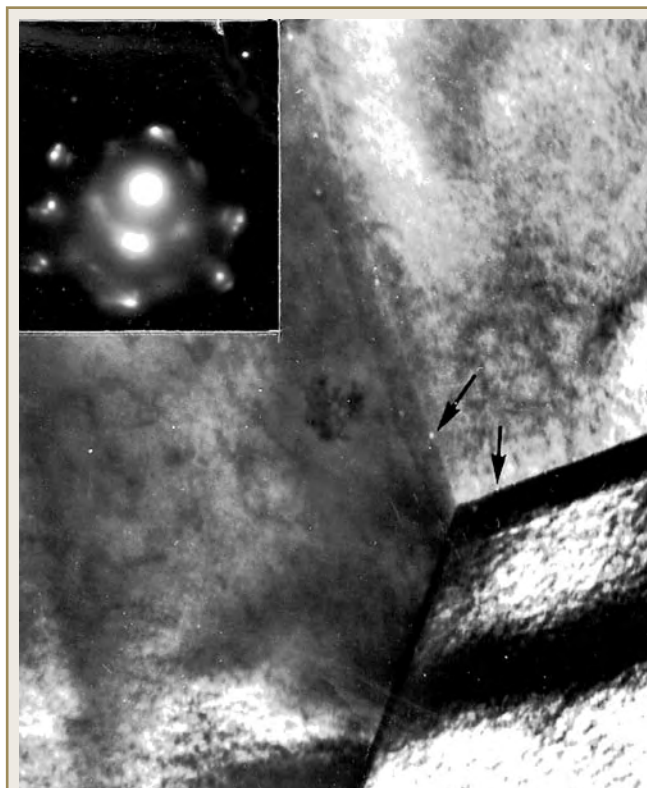
Electrons have short wavelengths (0.037 Å for 100-kV electrons) relative to atomic dimensions, creating small scattering angles. Because this scattering is very strong, fine detail can be seen at an atomic level in electron microscopes. Conventional microscopes

can measure these scattering angles for most low-atomic-number materials. But as atomic number increases, scattering and absorption increase, the transmitted electron beam diffuses, and the transmitted image information is lost. For reasonably thin foils, this scattering and absorption can be overcome somewhat by increasing the electrons’ accelerating potential. Thus, TEM’s ability to penetrate greater thicknesses of material at higher accelerating voltages is its most obvious advantage over conventional microscopy at 100 kV.

TEM has moved scientific research far beyond the stage of “looking at” materials with unrefined tools. With the invention of the electron microscope circa 1946 and its subsequent improvements through the mid-1950s, scientists began to see and resolve nanometer structures. The ability to observe such detail at the microstructure level

presented enormous research opportunities that advanced technologies in chemistry, environmental sciences, solid-state physics, geology/mineralogy, and metallurgy. The field of metallurgy, in particular, experienced one of its greatest expansions, because TEM studies confirmed or denied many long-standing theories. Defined by and based on fact instead of speculation, this new information in turn led to newer theories and definitive structure-properties connections. 

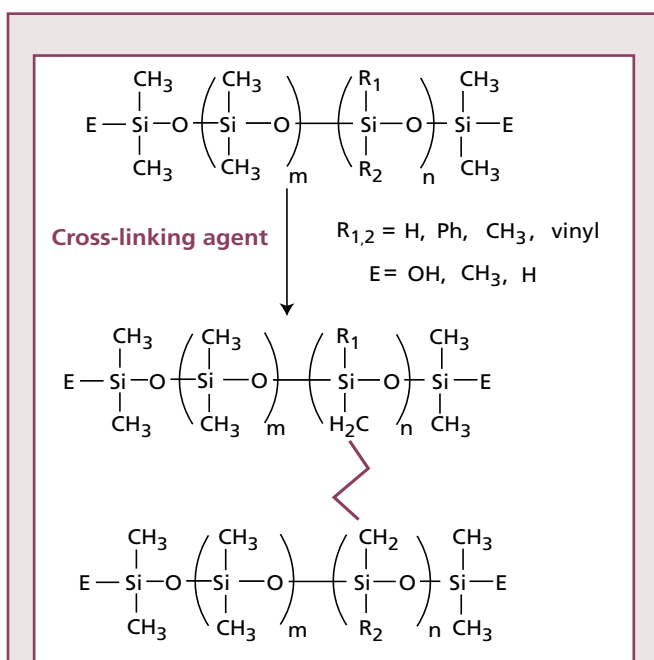
Point of contact:
Karl P. Staudhammer, 667-9333,
staudhammer@lanl.gov



Annealed delta plutonium alloyed with 1.5 wt% gallium. LANL’s first successful attempts were achieved on high-purity, delta-phase plutonium-239 alloyed with 1.5 wt% gallium. The plutonium had been stored in a vacuum since 1965. Arrows indicate helium bubbles that were produced from alpha decay of the plutonium that had been stored for nearly 17 years. Taken at LANL, this is the first TEM record of metallic plutonium.

Mechanical Properties of Nonporous Silica-Filled Silicones

This article focuses on the physical and chemical processes that influence the mechanical properties of silica-filled polydimethylsiloxane (PDMS). Silica-filled PDMS is commonly used in silicone bathroom caulk. Filled PDMS is of particular interest to the weapons community because it provides cushioning and mechanical support in nuclear weapons.



Generalized chemical structure and cross-linking reactions of silicone polymers. The structure inside $()_m$ in the diagram consists of a single PDMS unit, called a monomer. Each silicone chain consists of many PDMS monomers connected to form a long chain called a polymer. (When two or more different monomers are joined in the same polymer chain, the result is called a copolymer). The silicone copolymers can have a wide variety of end groups (E) and/or side groups (R_1, R_2) that may cross-link with other chains and interact with fillers. Linear silicones are liquids at room temperature. The number of monomers determines the polymer chain length and the resulting viscosity of the liquid. The number of side groups $()_n$ is related to the cross-link density or radiation resistance of the silicone. In the absence of filler, chemical cross-linking of multiple polymer chains forms an insoluble solid that has poor mechanical properties.

DEFINITIONS

Mullins effect—Decrease in stiffness (storage modulus) of filled rubbers that occurs after repeated stretching at higher levels of deformation than for the Payne effect.

Payne effect—Decrease in stiffness (storage modulus) of filled rubbers under cyclic deformation with increasing strain amplitude. Example: decrease in stiffness of automobile tire rubber caused by flexing. This phenomenon is not observed in unfilled rubbers.

reinforcement—Increase in strength and stiffness of a rubber upon addition of a filler.

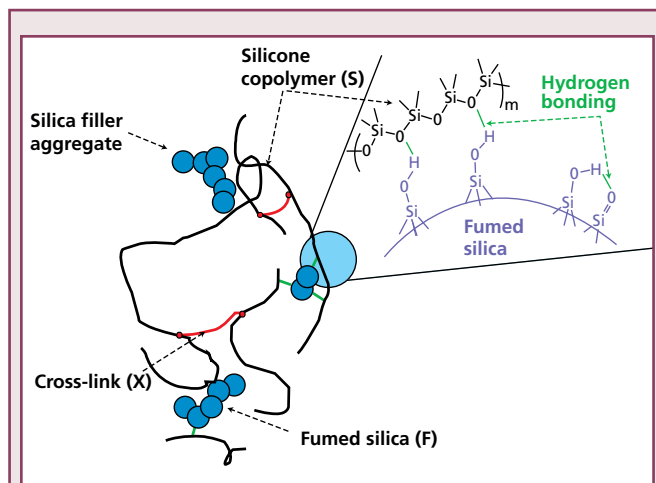
van der Waals force—Electrical attraction between molecules that causes them to “stick” together. This is a weaker attraction than hydrogen bonding.

The addition of small particles of filler (for example, carbon black, silica, or clay) to a polymer can dramatically alter the properties of the resulting composite. These filled polymers or polymeric binders are used extensively in applications such as tires, high explosives, structural foams, fuel cells, and high-performance nanocomposites. Although these materials have enormous commercial and strategic importance, there is little fundamental understanding of the physical and chemical interactions between the polymer matrix and the filler.

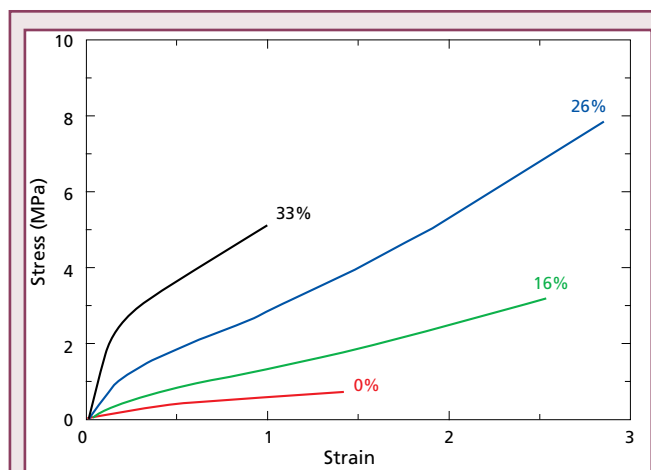
Adding filler to a polymer can substantially increase the composite’s strength. The filler can alter the orientation and conformation of the polymer’s molecular chains, which can impart properties to the polymer phase of the composite that are substantially different from those of the unfilled polymer. So what we know about the material properties of unfilled polymer doesn’t necessarily

apply to composites. Furthermore, the mechanical properties of filled polymers are unusually sensitive to deformation history—a composite that has been stretched, compressed, or twisted does not have all the same properties it did before deformation. The goal of our studies is to determine the structure/property behavior of filled polymers so that lifetime prediction models can be developed to predict composite behavior for extended periods of time.

While many different silicone formulations are used within the weapons complex, they all contain a siloxane copolymer, a filler, and cross-linkers. The PDMS polymer has a glass transition temperature of -120°C and melts at -40°C , resulting in a liquid at room temperature. The viscosity of the PDMS liquid is dependent on the length of the polymer chains and ranges from a light oil to a viscous gum. For high molecular weights, the uncross-linked PDMS molecules are like very long strings that are tangled and undergo irreversible deformation under their own weight. Silicone copolymers that



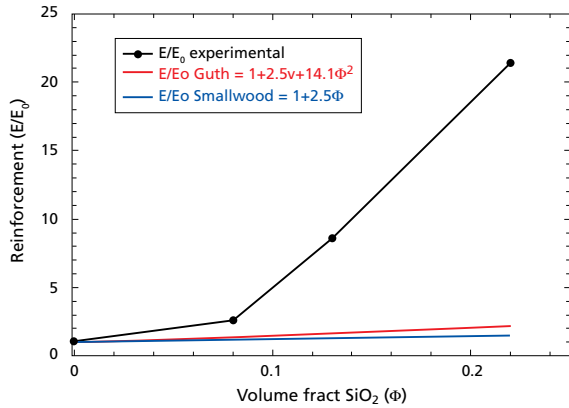
Physical and chemical processes involved with reinforcement of silica-filled silicones. Linear silicone copolymers (S) and fumed silica (F) are mixed and chemically cross-linked (X) to form an insoluble network. The fumed silica aggregates are dispersed but remain intact after mixing. Hydrodynamic and chemical interactions occur between the copolymer and the silica that strengthen the composite. The expanded view (right) shows hydrogen-bonding interactions between the surface silanol (Si-O-H) groups and the oxygen atoms in the silicone polymer chain (Si-O-Si). In addition, surface silanol groups can hydrogen bond with each other, potentially reducing the number of polymer/filler interactions and weakening the resulting material.



Observed relative increases in mechanical properties for PDMS composites to which various amounts of fumed silica have been added as filler. With no added silica (0 wt%), the silicone is a weak, gummy material. At 16 wt% silica, the PDMS has good elastomeric properties; the modulus (stiffness) of the PDMS increases by a factor of 2.5, the length at break doubles, and the stress increases by a factor of 4. Further increases in mechanical properties are observed in the composite up to near 26 wt% silica—but at higher levels the PDMS becomes brittle and the strain at break decreases. At these levels, the PDMS fractures rather than flows.

have PDMS as a major component incorporate chemical species to improve properties (e.g., phenyl groups for radiation resistance and hydrogen or vinyl groups for cross-linking sites). In the absence of filler, chemical cross-linking in the silicone ties the linear molecules into a network that improves the mechanical integrity of the material and makes the silicone a material that can be neither melt processed nor dissolved. If we add a powdered filler prior to cross-linking, we can further improve the mechanical integrity of the resulting composite.

Examples of silica fillers used within the weapons complex are diatomaceous earth, crystalline silica, precipitated silica, and fumed silica. The most dramatic change in mechanical properties is observed when amorphous fumed silica, such as Cab-o-sil® or Aerosil®, is utilized as a filler. The shape of fumed silica is difficult to characterize because the particles form wispy aggregates that are fractal in structure. These aggregates have a very high surface area ($\sim 200\text{ m}^2/\text{g}$), and the hydroxyl groups on the surface of fumed silica interact with the oxygen on the silicone polymer. These interactions by hydrogen



Comparison between calculated (Guth and Smallwood classic equations) and experimental results for the reinforcement (E/E_0) of PDMS with fumed silica. For all compositions, the predicted reinforcement from these models underestimates the observed values. With increasing amounts (volume fraction) of added silica, the deviation between these early models and observed values becomes increasingly pronounced.

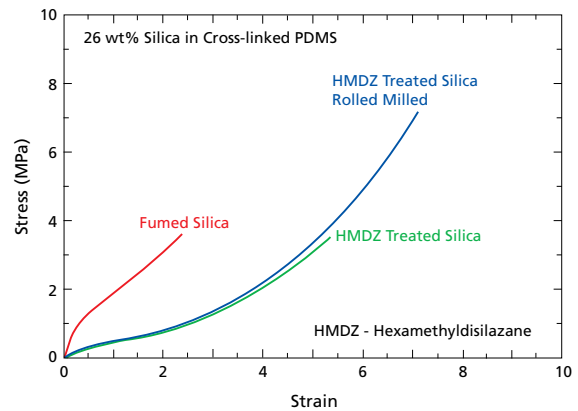
bonding are proposed mechanisms for the enhanced mechanical properties.

We prepare the composite by mixing a silicone gum and fumed silica in a dual axial mixer, followed by the addition of a peroxide cross-linking agent. We press this mixture into final shape and cure it at 115°C for 4 hours. We then post-cure the filled PDMS at 150°C for an additional 4 hours. For these samples, mechanical testing was done on an Instron Mechanical Tester in the tensile mode. The samples were cut into 1-in.-long dog-bone specimens and stretched at 10 in./min. The force upon stretching was recorded and then plotted against deformation to give a stress-strain curve.

One method of characterizing reinforcement is to compare the mechanical properties of the filled material with those of the unfilled polymer. Young's modulus is a measure of the material stiffness and is defined as the stress of a material divided by its strain at very small elongations (strains). With no fumed silica filler, cross-linked PDMS is a weak, tacky material that breaks easily. The addition of as little as 16 wt% fumed silica improves the strength of the silicone and significantly increases the reinforcement (E/E_0), where E and E_0 are the Young's moduli of the filled and unfilled polymer. Adding

fumed silica also improves the material's toughness by increasing the stress and strain to break. The modulus of the composite continues to increase with fumed silica concentration. The stress and strain at break go through maximum near 26 wt% silica. Between 26 and 33 wt% silica, the composite changes from an elastic to a leathery material, a change that is evidenced by an increased modulus and a decrease in the breaking stress and strain. For silica compositions above 33 wt%, the composite becomes brittle and difficult to process.

Early attempts to model the effect of fillers on the mechanical properties of elastomers were based on Einstein's equation describing the viscosity of a suspension. These hydrodynamic theories assumed that rigid spherical particles are dispersed in a continuous matrix (i.e., one with low volume fractions of particles). More than 60 years ago, Hugh Smallwood derived an equation for modeling the reinforcement (increase in modulus) by filler particles:



Comparison of the effects of different surface treatment and processing of silica on the tensile properties of PDMS containing 26 wt% fumed silica. The graph lines terminate at break.

Using untreated fumed silica results in a stiffer, more brittle composite. Treatment of the fumed silica to reduce chemical interactions between the polymer and filler results in a weaker, more extensible material. Processing the components in a roll mill more uniformly distributes the filler and produces a material that has greater extensibility and toughness. The improvement in mechanical properties due to roll milling is caused by the homogeneous dispersion of the filler so as to disrupt stress concentration points that cause premature failure.

$E/E_0 = 1 + 2.5\Phi$, where Φ is the volume fraction of the filler. Eugene Guth then introduced (in 1945) a second-order term that takes into account particle-particle interactions: $E/E_0 = 1 + 2.5\Phi + 14.1\Phi^2$.

The filler volume fraction can be calculated from the weight fractions $w_{f,p}$ by the equation $\Phi = (w_f/\rho_f)/(w_f/\rho_f + w_p/\rho_p)$, where ρ_f is the density of the amorphous silica filler (2.2 g/cm³) and ρ_p is the density of PDMS (0.97 g/cm³).

Although these models work for some moderately reinforcing fillers such as carbon-black-filled natural rubber, they significantly underestimate the reinforcement of fumed silica-filled silicones. In our tests, the observed moduli increase for silica-filled PDMS is 10 times greater for 33 wt% silica than that predicted by both the Guth and Smallwood equations. Although there are many newer models and hypotheses, there is still a lack of basic understanding of the theoretical mechanisms of reinforcement.

One commonly acknowledged mechanism of reinforcement involves polymer/filler interactions. Even though hydrogen bonding interactions between the oxygen in the silicone polymer and hydroxyl groups on the silica surface are responsible for the improved mechanical properties, these interactions can make it difficult to process even the uncross-linked composite.


One method of reducing these interactions is to treat (modify) the surface of the fumed silica with a chemical (hexamethyldisilazane) that inhibits hydrogen-bonding interactions. We studied the influence of silica surface treatment and processing on the tensile properties of fumed silica-filled PDMS. The filler content is 26% for all samples. For untreated fumed silica, the modulus of the composite is much greater than for the treated silica. However, the strain to break is greater for the treated silica due to weaker van der Waals interactions that allow for greater slippage of the polymer chains across the filler surface, thus reducing the mechanical stress in the sample.

Another variable affecting the mechanical properties of filled polymers is the dispersion of filler particles. Processing the polymer and filler in a roll mill more uniformly disperses the filler. This more uniform dispersion of the filler particles decreases localized

stress concentration points that may cause the material to fail prematurely, which increases the ultimate strength of the material.

We have demonstrated that filler content and its surface chemistry in filled polymers can have a dramatic effect on the tensile properties of the resulting composite. The mechanical behavior is further complicated when instead of simple stretching (tensile properties), the deformation mode is more complex (e.g., cyclic deformation). As observed in classical composites, these interactions produce phenomena known as the Mullins effect and the Payne effect.

Although these phenomena have been observed and utilized for many years, there is little fundamental understanding of how the physical and chemical interactions between the polymer matrix and the filler affect composite properties. Most of the current understanding has been derived from empirical correlations obtained from mechanical measurements where either the polymer, filler, or processing was manipulated. The lack of fundamental understanding is due to experimental difficulties with characterizing the surface chemistry and shape of the filler and with the lack of in situ monitoring techniques of the molecular orientation of the polymer during deformation of the composite.

Currently, we are developing novel in situ techniques that probe the molecular orientation and structure of the polymer in the composite at various length scales under different deformation conditions. Atomic force microscopy, scattering, and spectroscopic techniques are being utilized to correlate molecular structure with deformation amplitude, frequency, hysteresis, fatigue, and fracture for a variety of filled polymers. By understanding the effects of deformation on the molecular interactions at the polymer/filler interface, we can begin to develop science-based theories that predict the mechanical behavior of filled materials and binders and develop robust lifetime prediction models. A follow-on article discusses the use of atomic force microscopy to study filled polymers and presents the cyclic stress data. 

Points of contact:

E. Bruce Orler, 667-7317, eborler@lanl.gov

Debra A. Wroblewski, 667-7250, wroblewski@lanl.gov

Mechanical Properties and Filler Distribution in Silica-Filled PDMS

The mechanical properties of polymers can be significantly improved by the addition of particles of filler such as fumed silica. Formulations of silica-filled polydimethylsiloxane (PDMS) polymers exhibit a wide range of properties, from fluid to gum to flexible solid, depending on molecular weight, branching, filler, end groups, and cross-linking.

Filled PDMS has everyday, real-world applications in, for example, adhesives, oven-door gaskets, seals, and sponges, as well as in implantable devices and tubing used in medicine. The research discussed here focuses on PDMS formulations for weapons applications that require extreme flexibility, tensile strength, and compression-set resistance over a wide range of temperatures. The goal of this research is to obtain experimental data that can be used to develop realistic, predictive computer models that accurately simulate the behavior of filled PDMS.

To study mechanical properties and filler distribution in filled PDMS elastomers (rubbers), we fabricate “model” samples from purified materials with known composition and degree of cross-linking. The use of model samples allows our team to vary different parameters to study their impact on the elastomers’ mechanical properties, in particular correlating stress-strain behavior to filler content in the presence of cross-linking. We fabricate the samples under controlled conditions where a modification in fabrication procedure is a controlled variable. We modify only one parameter at a time so that we can correlate that change with changes in properties.

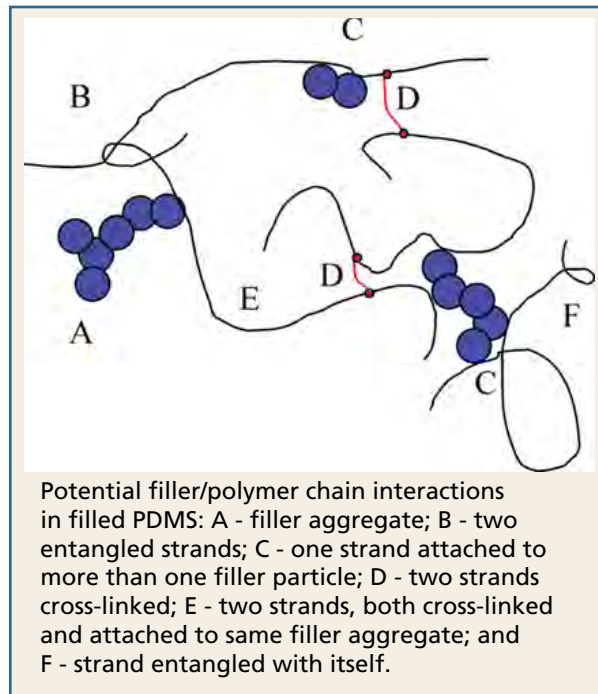
In addition to composition, the parameters we vary include tensile strain history and heat treatment. We determine whether or not the polymers continue to soften with subsequent tensile stress after an initial prestretch. Also of interest is whether aging alone or aging accelerated through heat treatment leads to recovery of the starting modulus (stiff-

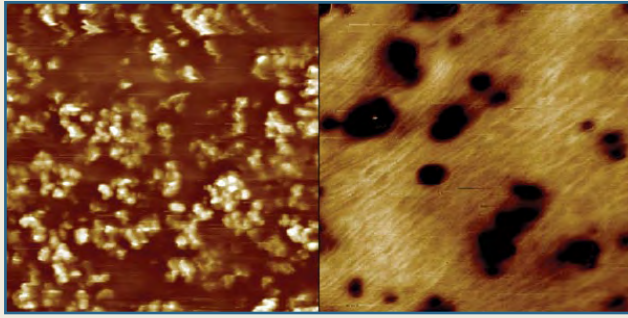
ness). We also explore the effect of one type of silica surface treatment on the mechanical properties, the degree of permanent set in the material, and the size and distribution of filler aggregates.

In particular, our experiments are designed to

- correlate mechanical properties of filled PDMS under tensile stress to filler content and filler surface treatment in the presence of cross-linking,
- explore the occurrence and persistence of a Mullins stress-softening effect, especially as it relates to time and heating,
- determine the degree of aggregation of filler particles and the uniformity of filler particle distribution, and
- determine the degree of permanent set for samples with an optimum filler content.

Polymers consist of molecules strung in long repeating strands, or chains. The primary factors that determine mechanical responses in particle-reinforced polymers are interactions between polymer and filler, cross-linking between chains, and entanglements within and among chains. The nature of





The contrast in the 1- μm x 1- μm phase images reverses when the cantilever tapping mode is changed from a "soft tap" to a "hard tap." The filler appears bright in the soft tap image (left), where the silica particle stiffness dominates, but dark in the hard tap phase image (right), where the larger AFM tip-sample surface area interaction with the soft matrix results in the soft material's appearing brighter.

the polymer-filler interactions in turn depends on physical and chemical interactions, including van der Waals interactions or hydrogen bonding caused by the presence of certain functional groups such as hydroxyl groups on the filler surface or polymer chain. In addition, the degree of aggregation of the filler particles determines the surface area available for attachment to the polymer chains.

We use a small tensile stage to characterize mechanical properties, and we use atomic force microscopy (AFM) to examine filler size, shape, and distribution in silica-filled polymers. AFM phase imaging exploits the sensitivity of an oscillating cantilever to local variations in the polymer's Young's modulus (stiffness). A tiny probe mounted on the cantilever moves back and forth across the sample surface, in intermittent (tapping mode) contact with the surface. Tapping mode AFM is used for soft samples like PDMS to minimize sample damage, which can happen when the tip is scanned across the surface while in contact with the surface. By oscillating the tip up and down, only intermittent or brief contact is made with the surface. The deflection of an oscillating cantilever up or down as the tip moves over the surface provides the structural image while shifts in the phase of the cantilever oscillation provide the local stiffness information. AFM is a powerful tool for mapping not only the size, shape, degree of aggregation, and distribution of filler particles but also the local nanoscale variations in mechanical properties.

To help us understand which interactions determine the tensile stress-strain behavior in filled PDMS, we fabricated test samples with filler content ranging between 0 and 50 parts per hundred (phr) by weight of the PDMS gum starting material while keeping the degree of cross-linking constant. We used AFM phase imaging and tensile stress-strain measurements to characterize samples with filler contents of 0, 20, 35, and 50 phr. One sample was made with 35-phr hexamethyldisilazane (HMDZ) treated filler. A small Fullam tensile stage instrument was used to measure tensile properties of 10-mm-long x 2-mm-wide, dog-bone-shaped samples cut from 0.5- to 1-mm-thick, pancake-shaped sheets of compression-molded materials. The samples were subjected to strains from 100% to 300%, depending on the filler content.

We took our measurements at a very low strain rate, i.e., only 0.1 mm/s, and we did not pull the samples to break in our study of tensile mechanical properties during cyclical elongation. After an initial pre-stretch, we stretched (strained) the samples multiple times to determine if the elastic properties continued to change from one measurement to another. In one case, a sample was stretched 100%, relaxed, then strained to 200%, relaxed, and finally strained to 250%. Also, six dog-bone specimens cut from the 35-phr filler pancake were subjected to an initial ~300% prestretch the same day. Different specimens were then retested at 1-week intervals up to 4 weeks, and one sample was retested after 26 weeks.

The stress-strain behaviors from the second elongations were then compared with the initial stress-strain behavior to determine if and to what degree these samples recovered their prestretch behavior as a function of time. A sample cut from a 35-phr PDMS pancake was tested before and after heating to 100°C for 18 hours to determine if heating accelerated recovery of the initial stress-strain behavior. Finally, latex paint was used to make a grid of fiduciary (reference) marks on three dog-bone samples of 35-phr PDMS. The spacing between these marks was measured before and after 300% elongation to determine the percentage, if any, of permanent set.

We collected sample topographic and phase images simultaneously. Samples were cut in cross-section

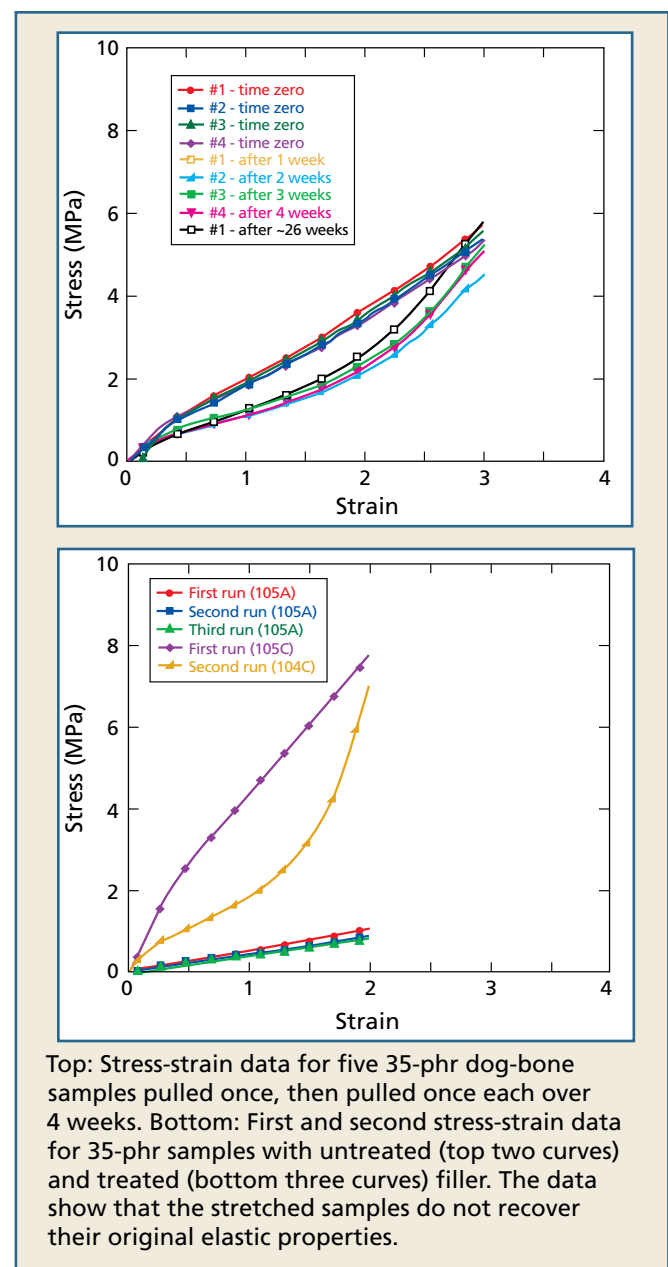
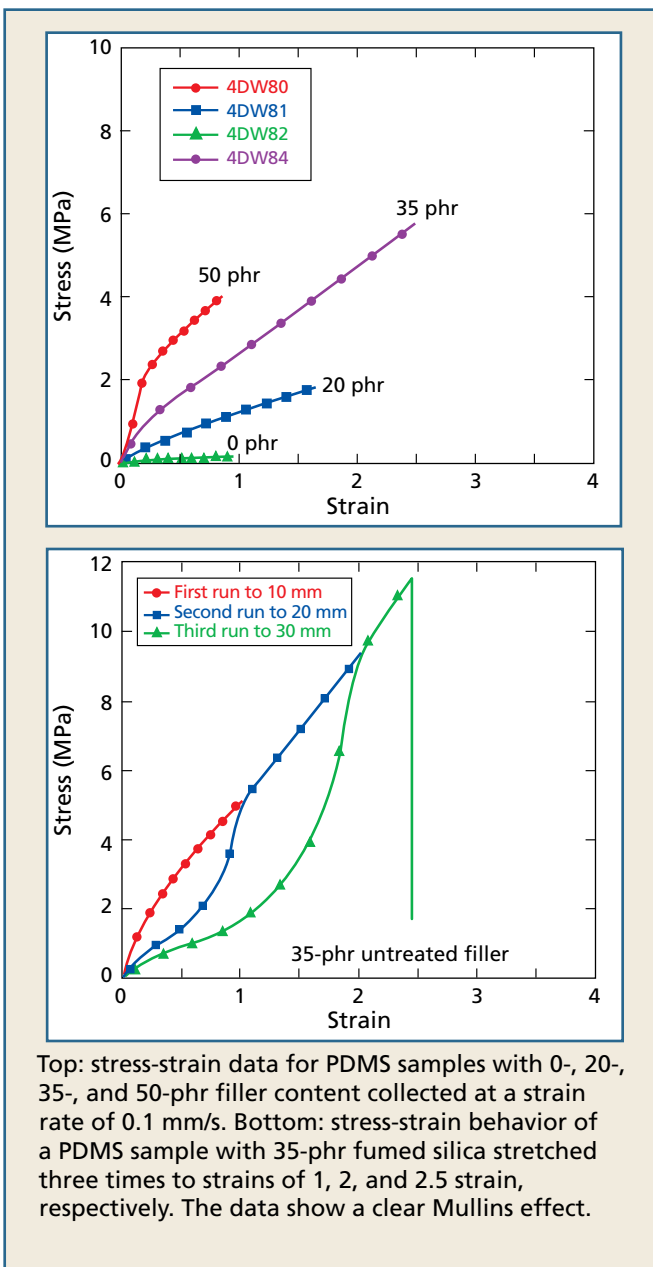
to access an “internal” surface for imaging. Simultaneously collected phase imaging was used to determine variations in filler distribution and degree of aggregation.

We addressed five issues in this work:

- the correlation between filler content and mechanical properties,
- the presence of a Mullins effect,
- aging effects (changes in mechanical properties with time and heat treatment),

- the influence of HMDZ surface treatment of the filler on mechanical properties, and
- the presence of permanent set, i.e., permanent deformation of the PDMS samples.

We saw a clear correlation between filler content and mechanical properties. Furthermore, the trend in the data is consistent with previously published results. Although the 50-phr samples had the highest modulus (stiffness), they easily fractured. In contrast, the 35-phr untreated filler samples evidenced the maximum combined stress and strain. These samples could be elongated to more than twice the



strain as the 50-phr samples and close to twice that of the 20-phr samples, which were softer but easily broken. The 0-phr samples were extremely elastic and difficult to mount in the tensile stage without breaking, let alone pull to 100% elongation.

A clear Mullins effect was seen for all samples made with untreated fumed silica filler. One sample with untreated 35-phr filler was stretched 100%, relaxed, then stretched 200%, relaxed, and finally stretched 250%. Although softening was initially observed, the graphs of the second and third elongation followed the prestretch curve once the strain reached the previously attained value. As for Mullins-effect softening in other samples, stress-strain behavior for samples pulled multiple times to the same strain did not exhibit continuous softening but rather overlapped the previous curve—that is, softening tended to stabilize with repeated stretching.

All dog-bone samples from the same 35-phr compression-molded pancake were prestretched the same day. One sample was tested after 1 week, a different sample was tested after 2 weeks, and so on for 4 weeks. In addition, one of the samples was retested after 26 weeks. All prestretch and second stress-strain curves overlapped within experimental error. No recovery of the original stress-strain behavior was observed. The sample that was heated to accelerate aging after the initial prestretch also showed no recovery of the initial modulus after the heat treatment.

The mechanical properties of the samples made with untreated filler were significantly better than those of samples made with the treated filler used in these experiments. The sample with 35-phr HMDZ-treated filler, although sustaining higher strains, had a lower modulus than the samples with 20-phr untreated filler. No obvious Mullins effect was seen for the sample with treated filler. Finally, a permanent distortion in shape was measured for samples with fiduciary marks. This “permanent set” amounted to approximately 3% to 6%.

Despite the careful mixing procedure used for samples with 0-, 20-, 35-, and 50-phr filler content to break up the filler aggregates and to disperse the particles uniformly throughout the material, we

KEY TERMS

aggregation—Cluster of primary particles.

branching—Outgrowth of chains from the main extended chain.

cross-linking—An atom or group connecting parallel chains in a polymer.

end groups—The final functional group at the end of a polymer chain.

entanglement—Ensnarement, intertwining, or intertwisting of polymer chains.

Mullins effect—Decrease in stiffness of filled polymers that occurs after repeated stretching at higher levels of deformation than for the Payne effect.

Payne effect—Decrease in stiffness of filled polymers under cyclic deformation with increasing strain amplitude. This phenomenon is not observed in unfilled polymers.

permanent set—Permanent change in shape.

phase imaging—A scanning proximity probe intermittent-contact imaging technique that maps the changes in the phase of the cantilever resonance that is sensitive to local differences in stiffness.

reinforcement—Increase in strength and stiffness of a polymer upon addition of a filler.

side groups—Functional groups extending off the main polymer chain.

strain amplification—Difference in strain in the macroscopic bulk properties of a composite and the localized (microscopic) stretching of a polymer chain upon deformation caused by the rigidity of filler particles within the matrix.

van der Waals force—Electrical attraction between molecules that causes them to “stick” together

observed that large aggregates were nonuniformly distributed across the sample surface for all samples except for the zero filler sample. The bright surface features in the phase images of the 20-, 35-, and 50-phr samples were not observed for the sample without filler, consistent with the association of these bright features with the silica filler. Although most of the filler appears to be aggregated, features <20 nm in diameter can be seen and are probably the fundamental filler particles.

continued on page 44

How Atomic Force Microscopy Works

Since the 1980s, scanned-proximity probe microscopy techniques have been powerful tools for obtaining atomic- to nanometer-scale 3-D surface structural information with little or no sample preparation. More recently, they have become indispensable for simultaneously obtaining maps of local variations in a number of different properties that can be directly correlated to compositional inhomogeneities, local variations in stress, and grain size and boundary effects. These properties control magnetic or charge domains, surface roughness, or, of particular interest here, local variations in mechanical stiffness.

Measurements are obtained using a tiny replaceable probe positioned very close to or on the surface of a sample and scanned over the surface. The type of probe tip and the imaging technique used determine the property to be measured. The replaceable probe is located at the end of a diving board-shaped cantilever that is mounted on the side of a piezoelectric tube. Then $\pm X$ and $\pm Y$ voltages applied to the tube's electrodes cause the tube to expand and contract, moving the tip back and forth across the surface in a raster pattern.

These computer-controlled scanning probe instruments are modular by design. They consist of a controller, which contains the instruments' operational electronics, a computer workstation containing the operating software, and a "probe," which holds the sample and probe sensors and contains the optical detection system or

electron tunneling preamplifier, depending on the nature of the measurement desired. Probes are interchangeably plugged into the controller.

There are three major classes of scanning proximity probe techniques: atomic force microscopy (AFM), also called scanning probe or scanning force microscopy; scanning tunneling microscopy (STM); and near-field optical microscopy (NSOM). The versatility of these collective techniques is due to their modular nature and the wide variety of available probe tips or sensors. Changing from AFM to STM operation simply amounts to changing a software switch, deciding which probe is to be plugged into the controller, and selecting an appropriate tip. A wide range of probe sensors is commercially available to suit the measurement needed.

AFM is one of about two-dozen closely related scanned-proximity probe techniques. AFM measures the attractive or repulsive forces between the probe's tip and the surface of the test sample as the probe is dragged very lightly across the sample surface. Because scanning probe methods all use a piezoelectric tube to move the tip over the surface, unlike other microscopes, the lateral and vertical resolutions are independent. Horizontal resolution is determined by the sensitivity of the piezoelectric tube to applied voltages ($\text{\AA}/V$). Vertical resolution is determined by the sensitivity of either the optical detection system or the electrical detection current (in the case of STM, where the tunneling current changes

by approximately a power of 10 per angstrom change in separation between metal tip and conductive sample). The size of the probe, the number of data points collected, and the sensitivity of the optical sensor, rather than diffraction effects, determine an instrument's vertical resolution. The result is that a 10-mm area can be scanned while angstrom-to-nanometer vertical resolution is maintained.

As the probe traverses the surface of a test sample, it moves up and down. This vertical deflection of the cantilever can be measured with picometer resolution. One effective way to measure this vertical cantilever movement as it follows the contours of the surface is to reflect a laser beam off the back of the cantilever onto a mirror, which in turn directs the beam onto a quadrature photosensor. Changes in position of the beam on the photosensor are used to measure the deflection as the cantilever moves up and down over surface features. This technique magnifies the probe's motions, producing very accurate measurements of material surfaces.

The AFM is operated in three different modes or combination of modes, i.e., the cantilever tip scans across the surface in contact with the surface, makes intermittent contact with the surface (TappingMode®), or scans above the surface in a combination of tapping and lift modes. The third method, not discussed in detail here, is used to measure long-range forces such as magnetic stray fields from magnetic data bits.

In contact mode, the probe touches the sample surface, much as a phonograph needle touches a record. However, unlike the phonograph needle, the cantilever has an extremely small force constant to prevent damage to the sample surface. In contact mode, AFM measures the probe's vertical deflection to generate a picture of the sample surface at the nanometer to atomic level. The probe's tip can also be scanned sideways to measure variations in local frictional properties by measuring how much the cantilever bends sideways (or twists). Metal-coated tips are used only for electrical or (if the metal is magnetic) magnetic properties. They are also used for electrochemistry, which is done under fluids. Otherwise, standard cantilevers are used in fluids.

Contact mode, using a metal-coated tip, measures local electrical properties such as piezoelectric response or tunneling current.

In many ways, tapping mode is a more powerful technique. The cantilever is oscillated at its resonance frequency, typically 50 to 300 kHz, so the probe tip is not dragged across the surface but rather makes intermittent contact with the sample. For that reason, tapping mode is less damaging for soft samples like polymers and biomaterials. It has the added benefit of allowing one to monitor shifts in the frequency or phase of the cantilever, which are sensitive to a number of properties, including local variations in mechanical properties. In fact, in tapping mode, researchers often monitor cantilever deflections to obtain

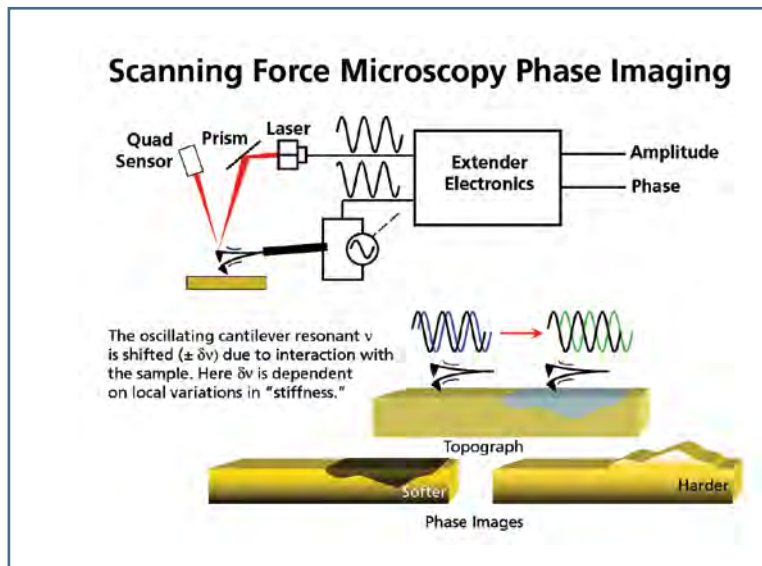
structural information and, at the same time, measure changes in the phase of the cantilever oscillation to obtain a one-to-one correspondence between structure and properties.

Phase imaging measurements map the changes in the phase of the cantilever resonance, which is sensitive to local differences in material stiffness. When the oscillating tip is scanned

this mode results in a larger surface interaction between the probe tip and the spongy matrix material and, therefore, results in a larger shift in the cantilever's resonant frequency or phase.

The last common operating mode of scanning probe operation is the combined tapping mode plus lift mode. In this method, the tip scans the surface in tapping mode, then the tip is lifted off

the surface at a distance defined by the operator. The tip is then scanned over the surface at a fixed distance above the surface by retracing exactly the same profile obtained from the surface scan. This method of operation is extremely powerful for obtaining either magnetic or electrical domain structure at the nanometer scale.



over samples such as filled polymers, which consist of relatively stiff filler particles in a soft polymer matrix, the phase shifts, depending on the Young's modulus (stiffness) of material on which the tip is tapping. This phase shift is due to an effective change in the force constant of the cantilever, which is affected by the tip's interaction with materials of different stiffness.

In general, if a "soft" tapping cantilever mode is used, brighter features in the AFM phase images correspond to material that is stiffer than their darker counterparts. The contrast is reversed for a "hard" tapping mode of operation where the cantilever tip is driven deeper into the "softer" polymer matrix material in the sample than it is into the stiffer silica filler. Using

These versatile scanning-proximity probe techniques provide high-resolution surface structural and related property information without tedious sample preparation. They operate under a wide variety of environmental conditions, ranging from ambient to ultra-high vacuum, controlled gas to liquid phase, or ultra-low temperatures to temperatures as high as over 1000°C. In many cases, changing from one technique to another only entails changing the type of tip, using a software switch, or selecting which probe is plugged into the controller.

Point of contact:
Marilyn Hawley, 665-3600,
hawley@lanl.gov

The Engineering Institute

Los Alamos enhances global security by ensuring the safety and reliability of the US nuclear stockpile, developing technologies to reduce threats from weapons of mass destruction, and solving problems related to energy, environment, health, infrastructure, and national security.

LANL and the University of California, San Diego (UCSD), are taking the unprecedented step of creating a multi-disciplinary education program and associated research agenda, the Engineering Institute, designed specifically to support LANL's mission of enhancing global security. This program is part of LANL's Engineering Science and Applications Division's comprehensive approach to mission-driven recruitment, training, retention, and research.

The program was initially supported by a 6-month, \$640,000 contract sponsored by LANL's Weapons Engineering and Manufacturing Directorate in collaboration with UCSD Jacobs School of Engineering. This funding supported student fellowships, curriculum development, and the purchase of laboratory equipment.

The Engineering Institute is a research-based educational system that focuses on technologies to detect damage and to predict the remaining useful life of engineered systems. This research will support critical infrastructure management in both the civil and defense sectors, including stewardship of the US nuclear weapons stockpile and maintenance of bridges, manufacturing infrastructure, and aircraft. (See the following article in this issue of the

Nuclear Weapons Journal, "Developing Structural Damage Prognosis Solutions.")

Over a 5-year period, LANL plans to hire approximately 300 engineers. This education initiative



As part of the Los Alamos Dynamics Summer School, a professor from UCSD works with an electrical engineering student on an experiment that was used to develop structural damage detection procedures using chaotic inputs.

will help provide the Laboratory with a well-trained workforce and create graduate-level, research-based education opportunities in mission-critical technologies. Beginning this past summer, four UCSD engineering graduate students were awarded Los Alamos fellowships. Eventually, as many as 30 students a year may be enrolled in the program. Twelve LANL staff members are currently taking graduate-level classes transmitted from UCSD

to Los Alamos over the Internet.

The curriculum will initially concentrate on structural health monitoring and damage prognosis and will include a strong emphasis on validated simulations. Through this program, students will take coursework in predictive modeling and simulation, sensing and diagnostics, and data interrogation. From a research perspective, students supported by the Los Alamos fellowships are actively participating in two current collaborations between Los Alamos and UCSD: detecting damage in the composite wings of the unmanned combat aerial vehicle and conducting research on degradation of composite-to-steel connections being considered for the next-generation Navy destroyers.

Currently, the Engineering Institute is located in the Los Alamos Research Park and has Internet access to UCSD classes. The Institute also brings

UCSD faculty to Los Alamos and has LANL staff serving as adjunct professors. In addition, the Institute will incorporate the existing Dynamics Summer School at Los Alamos. By integrating the Dynamics Summer School with the Education Initiative, LANL can begin to recruit top engineering talents during their junior year and then have a mechanism by which these students can stay engaged with LANL throughout their graduate academic careers. Finally, to support technology transfer, LANL staff and UCSD faculty have developed a specialty short course in structural health monitoring that is taught as part of a continuing education program for professional engineers from industries across the US.

“We believe this multidisciplinary research-based educational program directed toward the needs of the National Laboratories is one of the first of its kind. Although the program initially focused on structural engineering, the partnership has expanded to other key engineering disciplines at the Jacobs School including mechanical and aerospace engineering and electrical and computer engineering,” said Frieder Seible, Dean of the Jacobs School and Director of the Charles Lee Powell Structural Research Laboratories at UCSD. Seible added that the initiative leverages UCSD’s strengths in

large-scale structural testing, high-performance computing and visualization, and sensors and sensor networks with Los Alamos’ expertise and technical capabilities in damage prognosis, modeling, and materials characterization.

The LANL/UCSD Engineering Institute has the potential to become the first institute to focus on developing solutions to large-scale, multidisciplinary engineering problems of national importance. As LANL Director George “Pete” Nanos said, “...we will need the best and brightest from schools such as the UCSD Jacobs School of Engineering to take up the challenges of stockpile stewardship and develop the new technologies we need to fully understand these aging weapons systems. Although we will depend increasingly on the most powerful computers in the world to integrate weapons information, we won’t get the right answers in our models without the data these engineers will collect, analyze, and use to simulate damage states and useful service life.” [www](#)

Points of contact:

Charles Farrar, 663-5330, farrar@lanl.gov

Tony Andrade, 665-6989, andrade@lanl.gov

Timeline

- August 03: Associate Director for Weapons Engineering and Manufacturing provides \$640,000 to establish the Engineering Institute Initiative.
- September 03: Five students receive Engineering Institute fellowships at UCSD.
- September 03: Two joint defense-related research activities start.
- May 04: UCSD negotiates 2-year lease in the Los Alamos Research Park to house Institute.
- June 04: Engineering Sciences and Applications Division Office (ESA-DO) and the DOE Critical Skills Program fund Los Alamos Dynamics Summer School.
- September 04: ESA-DO funds five 40%-time education appointments for LANL early-career staff (e.g., MS-level engineers working on the Ph.D.).
- October 04: First graduate UCSD engineering course transmitted to LANL over the Internet.
- January 05: LANL staff teach first course transmitted to UCSD over the Internet.

Developing Structural Damage Prognosis Solutions

Damage prognosis (DP) is the process of predicting the remaining useful life of an engineered system, given some estimate of anticipated future loading. The DP initiative at LANL is developing and integrating new sensing hardware, new data interrogation software, and new predictive modeling software components that will be demonstrated and further refined through component- and system-level proof-of-principle experiments. This article discusses some of the issues that must be addressed and technical approaches that must be used to meet these challenges.

DP attempts to diagnose and forecast the performance of an engineered system by first assessing its current physical state, estimating future loading environments for that system, and, using both simulation and past experience, predict the remaining useful life of the system.

DP begins with three general questions:

1. What causes the damage of concern?
2. How should one assess and quantify damage?
3. Once damage has been assessed, what is the goal of the prognosis?

For each potential failure mode, the source of damage falls into three general categories: gradual wear (e.g., corrosion), predictable discrete events (e.g., aircraft landings), and unpredictable discrete events (e.g., hostile enemy fire, earthquakes).

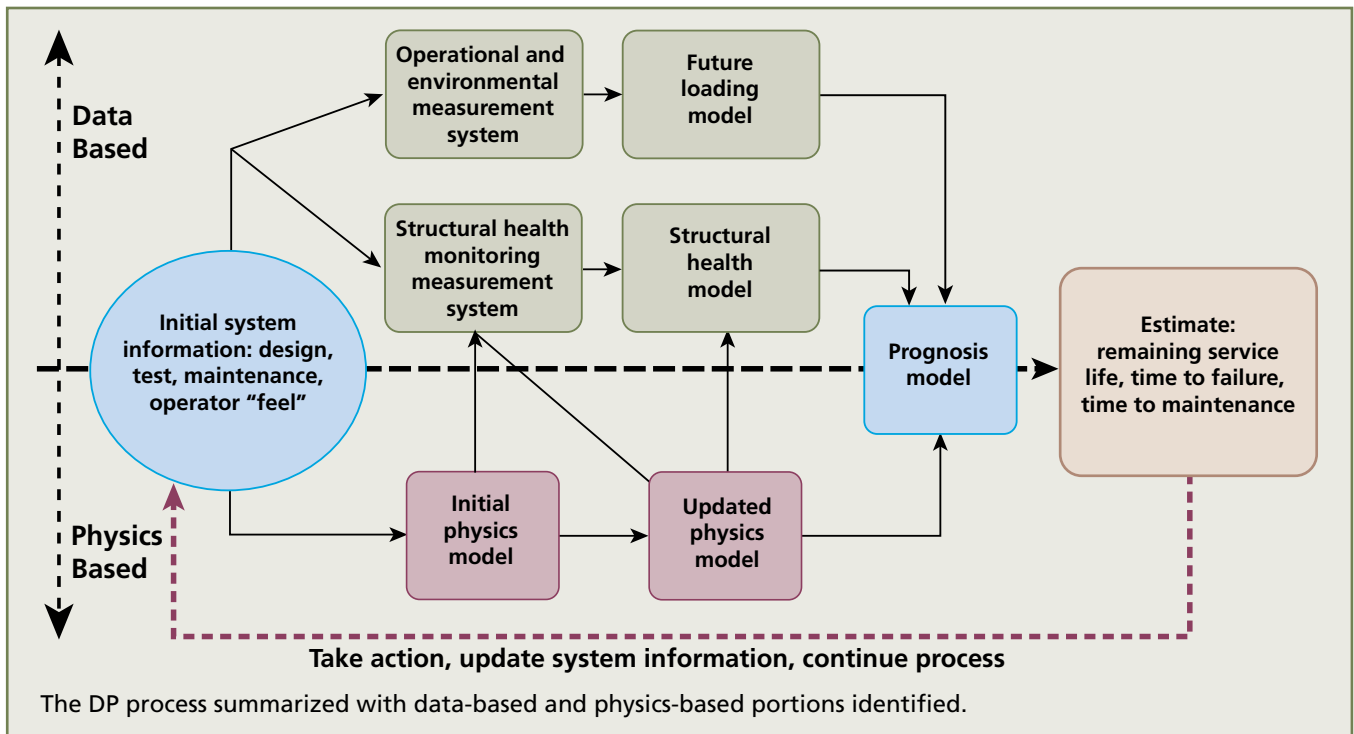
Next, we determine which techniques we should use and whether the damage assessment should be done on-line in near-real time or off-line at discrete intervals because this consideration strongly influences data acquisition, data processing, and computational

requirements of potential prognosis techniques. Assessment techniques can be classified generally as physics-based or data-based. However, we usually employ a combination of the two techniques. Finally, after assessing the current damage, we must determine the goal of the prognosis. Perhaps the most obvious and desirable type of prognosis may simply estimate how much time remains until system maintenance is required, the system fails, or the system is no longer usable.

Damage prognosis is a “grand challenge” for engineers.

We begin the DP process by collecting initial system information that we use to (1) develop physics-based numerical models of the system, (2) define the sensing system for damage assessments, and (3) identify additional sensors needed to monitor operational and environmental conditions. We use the physics-based models to define the necessary sensing-system properties (e.g., location, bandwidth, or sensitivity). As data become available from these sensing systems, we use them to validate and update the physics-based models. These data and output from the physics-based models then are used to assess current structural damage. Data from operational and environmental sensors are used to develop data-based models that predict future system loading.

For other DP applications such as seismic risk assessment, variability associated with the future loading model significantly impacts final prognosis uncertainty. The output of the future loading model, the structural “health” model, and the updated physics-based model are all input into a reliability-based predictive tool that estimates the remaining system life. Clearly, various models are employed, the data-based and physics-based portions of the process are



not independent, and the solution process must be repeated as new data become available.


Demonstration Problem

To simulate damage to an aircraft wing or fuselage in a laboratory setting, LANL's Structure/Property Relations Group conducted controlled projectile-impact experiments using the gas gun on a graphite/epoxy, fiber-reinforced composite plate. Then the damaged composite plate was subjected to steady-state cyclic loading. The general DP process requires finite element analysis (FEA) to train metamodels (reduced-order models) to predict impact location and velocity from sensor readings. FEA is then used to develop metamodels that can locate and quantify damage based on sensor readings and knowledge of the impact location and velocity. An additional metamodel is developed to predict fatigue damage accumulation based on the known initial-damage measurement. Prestablished threshold values for fatigue damage accumulation indicate system failure, and the metamodel predicts the time required to reach this threshold under the given loading environment.

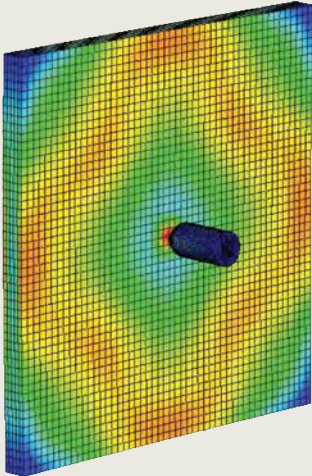
Physics-Based Models

Multilength-scale, physics-based models for damage initiation and propagation were used to develop a physics-based framework to analyze the composite

High-speed photograph of a nylon projectile impacting on an 8-ply, 15.24-cm-sq composite plate.



Simulation of damage to an aircraft wing or fuselage in a laboratory setting. A 185.5-g, 2.5-cm-diameter projectile was fired from a gas gun to impact on a graphite epoxy, fiber-reinforced composite plate. FEA was used to develop analytical computer predictions of the stress contours produced by the impact. The damaged composite plate is then subject to cyclic loading to assess how many fatigue cycles can be applied before the impact damage becomes critical.



plate's response to impact and fatigue loading. To correctly address modeling issues associated with the composite material's response, we use a novel multiscale finite-element (MSFE) approach that is based on a generalized, nonlinear, multilength-scale plate theory. This theory accounts for the initiation and evolution of delaminations through the use of cohesive zone models.

First, individual laminas are modeled using ply-level homogenization techniques and assumed linear elastic behavior for the fibers and matrix. Currently, nonlinear homogenization models are being integrated into the MSFE framework. This approach correctly predicts damage to the material microstructure, accurately determining history-dependent deformations and fracture behavior at the fiber level. It also predicts the bulk response of the lamina. A strong form mathematical solution replaces the current variationally derived theory. That approach satisfies the traction continuity conditions between lamina in a strong sense, which increases the ability of the plate theory to provide high-fidelity predictions of delamination behavior.

System Sensing

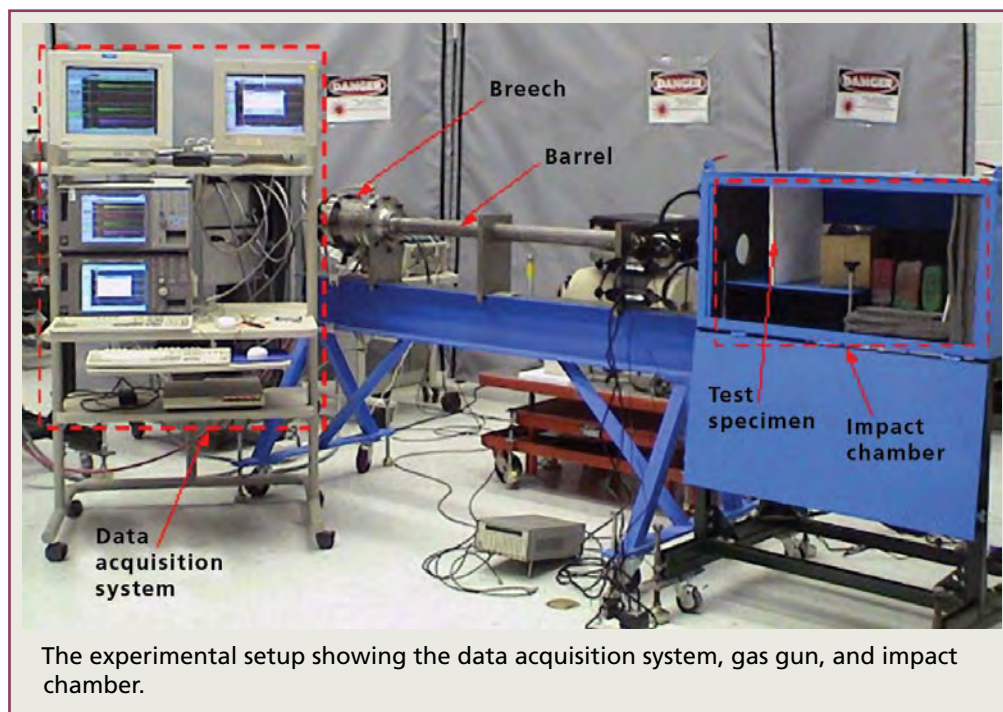
The proposed sensing strategy has three major parts: (1) active, local sensing to monitor both onset and growth of damage, (2) passive global sensing to assess system-level response and loading conditions, and (3) a sensing system design methodology to maximize the observability of a given failure mode and degradation mechanism. Initially, the hardware aspects of this work focus on using recently developed active piezoelectric (PZT) sensors and conventional accelerometers.

PZT sensors/actuators are inexpensive (approximately \$5/PZT patch), generally require low power, and are rela-

tively nonintrusive. Three documented successful methods in the areas of active, local-damage sensing using PZTs are (1) the impedance-based damage detection method, (2) the Lamb-wave propagation method, and (3) the time-reversal acoustics method. Here the term active sensing refers to the fact that PZT patches are used as both a sensor and an actuator. As an actuator, the PZT can produce a known wave input into the structure that is designed to enhance the damage identification process. These methods operate in the high-frequency range (typically above 30 kHz) where measurable changes occur in structural wave-propagation characteristics for incipient damage associated with crack formation, debonding, delamination, and loose connections. After detecting structural damage, the PZT sensors acting in the passive mode can assess the influence of damage on system-level performance and provide data to predict future system life.

Data Interrogation

The main issues for data interrogation are converting sensor data into system damage information, developing data-based models for future loading environments, validating and updating predictive physics-based models, and fusing numerically-simulated and experimental data to support final DP decision-making. Data interrogation encompasses many aspects of signal processing, machine learning



techniques, statistical pattern recognition, and data management.

The data interrogation process must be integrated with other parts of the DP process. First, model update and refinement requires use of experimental test data to adjust and validate the numerical model. In this process, data interrogation condenses massive numerical data and extracts features from physical measurements for comparison with features extracted from numerical data. The statistical pattern-recognition component of the damage diagnosis process defines damage-sensitive features and formulates statistical procedures to determine the existence, location, and extent of damage. DP is the result of integrating the current system state assessment (determined from the damage diagnosis process), estimated future loading information, and the predictive capability of the previously refined model. Future loading can be forecast using various data-driven statistical modeling techniques. Then a decision analysis process, similar to the one in the damage diagnosis, is designed to synthesize all this information and make the DP. Six data interrogation methods are needed for this process: data validation, feature extraction, data normalization, characterization of feature distributions, statistical inference for decision-making, and prediction modeling for future loading estimates.


Metamodels for Damage Prognosis

High-fidelity, multiscale physics models can provide unprecedented predictive capability for damage initiation and evolution, but these models are not suitable for onboard, near-real time DP assessments. Metamodels are being developed based on outputs from the large-scale, physics-based models. Metamodels capture the relationship between inputs and outputs without providing a detailed description of the underlying physics and system geometry. Examples of metamodels include polynomials and neural networks. Metamodels can run on micro-processors and so can be directly integrated with a sensing system and embedded onboard the structure. Developing a metamodel requires the ability to validate the physics-based models and to quantify and propagate uncertainty through these models.

Reliability Analysis for Damage Prognosis Decision-Making

DP forecasts are performed in the context of reliability analysis. For the composite plate demonstration problem, a probabilistic reliability analysis shows how many additional fatigue cycles can be applied before impact-induced damage becomes critical. This analysis begins by identifying the failure modes (such as delamination) for the composite plate and the random variables that contribute to these failure modes (e.g., projectile velocity, ply orientation angles, homogenized elasticity parameters). To calculate the probability of failure, the joint probability density function that relates these variables to the probability of failure must be integrated across all random variables for the failure region. Because closed-form mathematical representations of the failure region are generally not available, integration must be approximated by applying Monte Carlo sampling or approximate expansion methods to the previously identified metamodels.

In the real world, DP can be applied to all types of aerospace, civil, and mechanical systems. To date, the only successful DP application has been predicting the life of rotating machinery. Successful applications of rotating-machinery DP exist because extensive data sets are available, some of which include monitoring the machines to failure. Also, the damage location and damage types, as well as operational and environmental conditions, are often well known a priori for this application.

DP is a grand challenge for engineers because of the multidisciplinary nature of the technology needed to obtain robust DP, the broad applications of this technology to civilian systems (e.g., offshore oil platforms, commercial aircraft, amusement park rides) and defense systems (NNSA weapon systems and conventional military hardware and weapons), and the tremendous life-safety and economic impacts that this technology can provide. 

Points of contact:

Charles Farrar, 663-5330, farrar@lanl.gov

Francois Hemez, 663-5204, hemez@lanl.gov

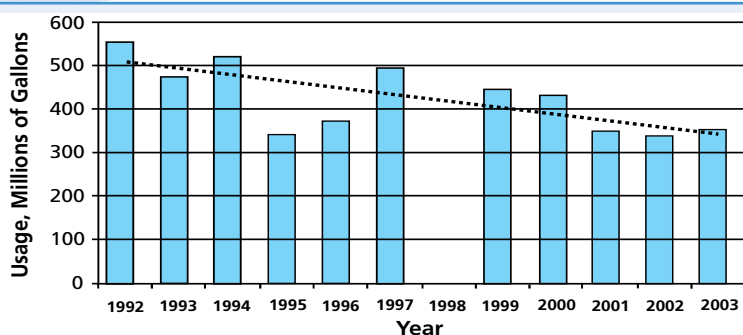
Water Conservation: Avoiding a Crisis

When Los Alamos was selected as the site of the research laboratory for the Manhattan Project, J. Robert Oppenheimer had no idea that the site's limited

water supply might someday restrict the amount of work that could be conducted here. Since 1943, LANL's size and scope have increased dramatically, while the availability of adequate water has remained tenuous, in part because the state has experienced drought conditions for the last several years. However, the Laboratory is working proactively to prevent a water shortage and ensure an adequate supply of water for both current and future programmatic work.

The Laboratory uses water for many purposes, including regular operations, domestic use, landscaping, and temperature control. Laboratory water use also is tied to energy use: 58% of the Laboratory's water is pumped through cooling towers. This practice is especially significant for the nuclear weapons community because the largest cooling towers, by volume of water consumed, are those of LANSCE at TA-53, the TA-3 towers associated with the Laboratory's large computer facilities (Central Computing Facility, Data Communications Center, Nicholas C. Metropolis Center

for Modeling and Simulation), and the TA-3 power plant. LANSCE alone utilizes one-third of LANL's allotted water.



Source: 2003 Pollution Prevention Roadmap (LA-UR 03-9021).

Yearly water usage. Beginning in 2001, water usage at LANL stabilized at approximately 350 million gal./year as the Laboratory undertook ongoing water conservation projects such as repairing almost 100 miles of leaky, aging pipe; improving and replacing cooling towers; and reusing sanitary wastewater. No reliable data are available for fiscal year 1998 because in that year, operation of the Los Alamos water supply and distribution system was transferred from DOE to Los Alamos County.

LANL currently is allocated no more than 542 million gal. of water per year—roughly the equivalent of all the summer water in the Rio Grande flowing past Otowi Bridge for a continuous period of more than 49 hours. But in 2000, the institution was already using approximately 430 million gal. each year, or

approximately 80% of the Laboratory's available resource. And LANL's water use was projected to increase 30% by 2005 as new projects and facilities became operational. LANL's projected water need for 2005 was 655 million gal./year, more than 110 million gal. above its allocation. That's enough water to cover every square foot of usable space in all LANL facilities to a depth of 2.5 feet.

Proactive Conservation Projects

To avoid a crisis, the Laboratory began to address its potential water problem through project- and area-specific water-conservation projects. These efforts included inspecting and repairing the Laboratory's 100-mile-long, 30-year-old water delivery system, reusing wastewater, and upgrading cooling-tower

operations. The result: by 2001, water usage at LANL stabilized at approximately 350 million gal./year.

Historically, the Laboratory lost approximately 16% of its water allotment through leaks in the delivery system, much of which is composed of aging polyvinylchloride, cast iron, ductile iron, steel, and asbestos cement pipes. Now FWO-UI inspects the water-supply pipes to identify leaks, tracks water use, and oversees upgrades and repairs to the infrastructure. The result: FWO-UI has helped the Laboratory avoid the loss of approximately 10 million gal./year of valuable water.

LANL will maintain water usage at or below its current allocation.

In 2001, as part of its water-treatment process, the operators at the Radioactive Liquid Waste Treatment Facility changed one of their operating processes by substituting nonpotable process waters (sand filter effluent) for clean tap water when they mixed clarifier chemicals, lime, and ferric sulfate. The result: in addition to saving 650,000 gal./year of potable water, these changes decreased workload and led to eliminating 2000 gal./day of effluent.

Cooling Tower Improvements

At LANSCE, the Laboratory has constructed effective new cooling towers and improved the cooling-tower control systems. The facility also began updating water-treatment methods so that water in the cooling towers can be reused. These LANSCE projects reduced water consumption by several million gallons each year. The Laboratory also installed improved cooling-tower control systems at TA-35 and is making similar improvements to the cooling towers at TA-48. The new Metropolis Center was designed and constructed with modern, efficient cooling-tower control systems already in place.


SERF

A major constraint on the cooling towers' water efficiency is the silica concentration in the cooling water. The concentration of silica in local groundwater is approximately 88 parts per million (ppm). Because silica precipitates out and fouls heat-

exchanger surfaces at roughly 200 ppm, silica concentrations must be below that level in groundwater used in Laboratory cooling towers. Until recently, the Laboratory controlled silica concentrations in the water by using it for no more than 1.5 to 2.0 cooling cycles (cycles of concentration). However, the Laboratory this year brought on-line the Sanitary Effluent Reclamation Facility (SERF) that allows the cooling-towers to reuse the water for as much as two more cooling cycles.

SERF also treats sanitary effluent from LANL's domestic wastewater treatment facility at TA-46. This additional processing allows reclaimed sanitary effluent to be used as cooling-tower makeup water for the new Metropolis Center. SERF uses membrane processes to remove silica, enabling the cooling towers to run at a minimum of 4.0 cycles of concentration using reclaimed water instead of potable water. The reuse of sanitary wastewater, coupled with improved cooling-tower controls and use of cooling-tower water at higher cycles of concentration, is expected to further reduce LANL's water consumption by about 40 million gal./year—approximately the amount of water that would fill 61 average community swimming pools.

Commitment to Mission

Because responsible water use is critically important to northern New Mexico, LANL is committed to maintaining its water usage at or below its current allocation of 542 million gal./year. To ensure adequate water supplies for its current and future programmatic work, the Laboratory not only is working to sustain current conservation initiatives, but also is developing and implementing technologies that will further reduce its vulnerability to a limited water supply. The Laboratory is committed to sustainable, improved water-use practices that ensure its water resources are adequate to meet DOE's mission of stockpile stewardship and the missions of other Laboratory projects. 

Point of contact:

Monica Witt, 667-8626, mwitt@lanl.gov

Classified Removable Electronic Media: A Proactive Approach

The media spotlight has recently focused on the management of classified removable electronic media (CREM) holdings at Los Alamos and throughout the entire DOE Weapons Complex. What is CREM and why do there appear to be so many challenges handling it?

Within the DOE Weapons Complex, all classified matter must be identified and protected. Certain types of classified matter have a high level of common (shared) usage that results in an associated increase in the level of risk—more users create more opportunities to lose or misplace information. With the prevalence of electronic media, CREM is a prime example of a commonly used information format that is highly risky.

Following CREM mismanagement episodes at LANL during the last 3 years or so, UC standardized the definition of and practices for handling accountable classified removable electronic media (ACREM) for UC-managed LANL and LLNL. ACREM definitions and practices are stated in the University of California Policy on Accountable Classified Removable Electronic Media, effective March 3, 2004:

Classified electronic media are those materials and components manufactured to provide nonvolatile storage of classified digital data that can be read by a computer. “Removable” refers to such media that are

- designed to be introduced to and removed from the computer without adverse impact on computer functions, or

- separated from the computer for any reason, or
- portable electronic devices.

Media included in this CREM definition are computer hard drives, floppy disks, CDs, various types of tape cartridges, and even the solid-state memory found in digital cameras. The classification level of the information contained on the media is generally at the Secret Restricted Data level and above for the CREM to be considered accountable.

Los Alamos has developed more accurate, institutionally based systems and procedures to handle CREM, creating a more secure environment for classified information.

To compensate for a high level of handling risk, CREM is tracked through a detailed accountability system. CREM are assigned unique identifiers such as manually affixed bar codes or vendor-provided serial numbers. The accountability system, containing standardized data fields, serves as a registry of the items, their location, and their status history (creation, transfer, destruction). Special multi-person inventory teams, consisting of local managers, classified library custodians (CLCs), and neutral parties, conduct physical inventories periodically (at a minimum, a 100% inventory of all accountable CREM at LANL is performed annually) to ensure that all CREM recorded in the automated system is actually physically present and that all physically present CREM is recorded in the system.

The acronyms CREM and ACREM are often used interchangeably, but they have somewhat different meanings. ACREM refers to “accountable” CREM. Also, CREM does not have to be tracked in an accountability system if it has layers of physical protection and its removal can be quickly detected by electronic monitoring capabilities. Engineered approaches have a much higher level of reliability than human administrative systems. Because an engineered system substantially reduces the risk of inadvertent loss, CREM does not need to be accounted for in an administrative system. This segmenting of CREM accounting allows more concentration on the riskier components that are not under an engineered system.

Los Alamos has thousands of pieces of ACREM that must be protected and handled. In light of recent incidents, the current distributed model of handling ACREM—approximately 700 storage locations and almost 4,500 people involved in using and storing individual pieces of ACREM—is being replaced with a centralized system known as the “classified media library” model. This library model establishes a few locations for ACREM storage and then uses a “check-out, check-in” process for users who need ACREM at their desks or work areas.

Within the near future, LANL will have approximately 20 media libraries in vaults or vault-type rooms. These libraries will follow the Laboratory’s institutional procedures for creating, checking out, transferring, and destroying ACREM. This standardization, in itself, significantly decreases the chances of administrative error.

Day-to-day management of the media libraries will be entrusted to CLCs, who will be the owners of record of ACREM. All CLCs will be part of the Security and Safeguards Division at Los Alamos, which expects that consolidating the CLCs into one organization will result in more positive, more proactive, better-trained employees, and a more consistently administered and protected ACREM environment.

The ultimate answer, however, to controlling ACREM at an institutional level is to eliminate the need for it. The Laboratory is beginning an aggressive 2-year initiative to extend its classified network to every facility that does classified work. Use of the classified network will virtually eliminate the need for removable computer media.

As a byproduct of the move to media-less computing, the Laboratory will need to securely destroy thousands of pieces of ACREM. Using a novel idea from a staff member, the Laboratory is establishing a new facility that will alleviate some of the fear of mistakenly destroying information, a common thread in at least two of the recent CREM episodes at Los Alamos. A new CREM Staging and Storage Center (CSSC) will accept ACREM intended for destruction, then inventory and store the ACREM for up to 6 months. The CSSC will then begin physically destroying amounts of ACREM equal to that of new ACREM being delivered. This builds a “lag” time between when the ACREM is identified and moved out of the work environment and its actual destruction. During this time, several inventories will be conducted in the work environment, allowing for corrective action if the wrong ACREM was inadvertently sent for destruction.

Although the spotlight on CREM at the Laboratory has been harsh, the long-term outcome is positive. Los Alamos has developed more accurate, institutionally based systems and procedures to handle CREM, creating a more secure environment for classified information. The adjustments needed to integrate this new way of using CREM are just beginning—and there will, no doubt, be growing pains. **NWJ**

Point of contact:

Donald Willerton, 667-2888, dxw@lanl.gov

The Integrated Work Management Process

In a continuing effort to not injure people or the environment or compromise the security of the nation while accomplishing its mission, Los Alamos National Laboratory has implemented an integrated work management (IWM) process. The nine-step IWM process is illustrated in the diagram below.

Laboratory leadership determined that a fully integrated and truly graded approach to work management that would incorporate project management, quality management, safety, security, and environmental protection would address operational issues and achieve operational excellence.

Work performance requirements at LANL had evolved into several diverse, organizationally dependent processes. For the most part, these processes were inconsistent and inefficient. As a result, the Associate Deputy Director for Operations and the Division Director for Performance Surety directed that a committee be formed to address these inconsistencies and establish a new IWM structure. The proposal was then presented to the Laboratory's Director and the DOE-LASO Manager, who then chartered the Integrated Work Management Committee (IWMC).

The IWMC was chartered to

- improve and integrate work management practices, requirements, and procedures from integrated safety management (ISM), integrated safeguards and security management (ISSM), safe work practices, facility management work control, project management, conduct of operations, quality management, and environmental management systems;

- provide a single process for doing all work safely, securely, and in environmental compliance at LANL;
- provide managers and workers with the necessary tools to make decisions and successfully implement IWM across the Laboratory; and
- monitor and assist the implementation and continuous improvement of these processes.

The term “hazard” is used to mean any source of environmental, safety, or health danger or any safeguards and security threat or vulnerability.

The IWMC established the LANL IWM process for doing work in a manner that protects people, the environment, property, and the security of the nation. The process is designed to accommodate work ranging from a preventive maintenance operation with a set of well-defined steps to a large, one-time research experiment. The term “hazard” is used to mean any source of environmental, safety, or health danger or any safeguards and security threat or vulnerability. Similarly, the term “controls” is used to convey the mechanisms, processes, procedures, and preventive measures used to reduce the risks posed by these hazards.

IWM defines the requirements for implementing the five-step process associated with ISM and ISSM and directly supports the LANL Environmental Management System at the activity level. While implementing these five steps (define the work, identify and analyze hazards, develop and

implement controls, perform the work, and ensure performance), IWM emphasizes the following:

- management and worker accountability;
- applying the worker's knowledge and experience;
- providing integrated, worker-friendly documentation that includes defined work tasks/steps linked to specific hazards and unambiguous controls;
- identifying a single person-in-charge for each work activity;
- providing independent oversight and facility coordination;
- validating, releasing, and closing out work activities formally; and
- providing feedback and continuous improvement.

The two most important aspects of this process are the direct involvement of workers in controlling the risks and the accountability of responsible division leaders (RDLs) and responsible line managers (RLMs) for safety, security, and environmental protection.

Workers must be actively engaged throughout the IWM process to provide the practical, expert knowledge needed to fully identify hazards and to ensure that controls are effective and procedures are workable. Workers must perform their work within established control systems and continually evaluate these systems to ensure they are adequate for the work they perform.

The IWM process allows management judgment, tailoring, and decision-making to address the broad range of hazards and complexity of work at the Laboratory.

The RDLs and RLMs must

- establish processes to implement the requirements of IWM;
- determine the adequacy of controls to mitigate the risks;
- determine the competence and commitment of workers to perform work in a safe, secure, environmentally responsible manner; and
- assess operations to identify needed improvements.

In certain cases, the adequacy of controls must be evaluated and approved by institutional support organizations: for example, the Biosafety Committee; Pressure Safety Committee; the Health, Safety, and Radiation Protection Division for radiation work permits; the Risk Reduction and Environmental Stewardship Division for environmental permits; and the Security and Safeguards Division for vaults, classified computing, alarms, and access control systems. [WWW](#)

Point of contact:

Craig Taylor, 665-3545, eggus_taylor@lanl.gov



Point of View, continued from page 1

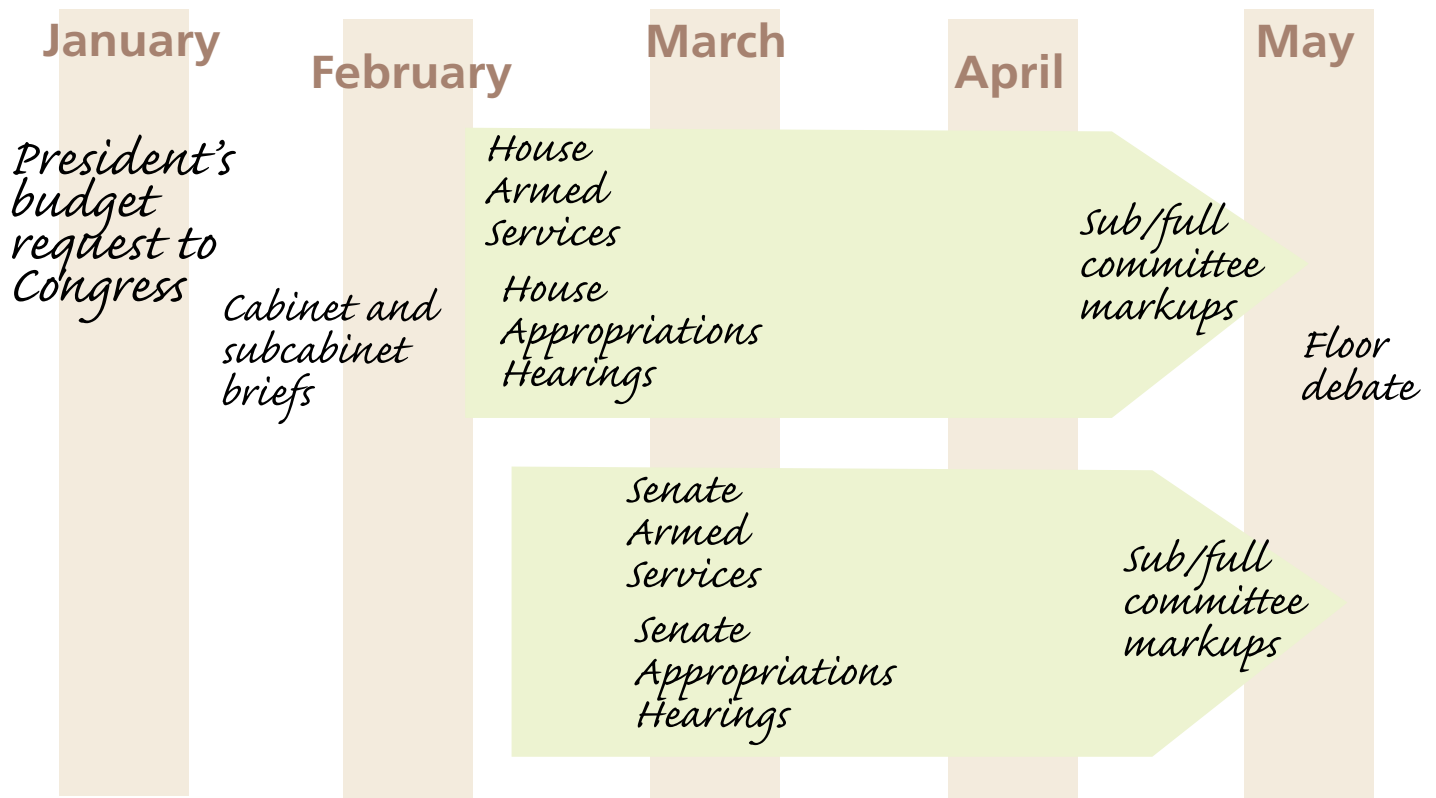
record), the subcommittee begins a detailed budget review. The subcommittee makes policy and funding recommendations to the full committee for its consideration. The full committee sets aside several days to debate and vote on the proposed funding levels and policy initiatives from each subcommittee and considers amendments offered by members.

Once approved at the committee level, the legislation goes to the full House and Senate for debate. Because of the large size of the House (435 members), the timing and scheduling of debate in the House is controlled by the powerful Rules Committee, which sets the amount of time and the number of amendments that will be considered. Because the Senate is a much smaller body (100 members), a unanimous consent agreement is proposed by the majority leader or floor manager of the measure (Sen. Warner for the Armed Services Committee), which reflects negotiations among senators interested in the measure. The agreement outlines when debate begins, the amount of time allocated to debate, and the germane amendments.

In 2003 and 2004, both the House and Senate vigorously debated the merits of allowing the laboratories to pursue the Stockpile Services Advanced Concepts

Program and the Robust Nuclear Earth Penetrator (RNEP) study, and whether the United States should improve its test readiness posture. Amendments were offered during committee markup and during floor debate to eliminate funds for these efforts. The House defeated the amendment proposed by Rep. Tauscher (D-CA) that would have transferred \$25M to conventional programs to deal with hardened and deeply buried targets and the Senate defeated an amendment proposed by Sen. Kennedy (D-MA) to eliminate all programmatic funding for these two initiatives. Text of debates can be found in the Congressional Record. The House debate occurred May 20 and the Senate debate June 15, 2004.

Inevitably, a conference committee made up of members from both committees and parties must resolve policy and funding differences. Conferees meet, usually in July, and produce a conference bill by early September. The Executive Branch works closely with committee staff (majority) throughout the entire process to sustain the President's budget and policy objectives. The conference measure must then be approved, without amendment, by both chambers of Congress before it is sent to the President for his veto or approval. If vetoed, the measure



is returned to Congress, which must either revise the legislation to address the President's specific objections or override the veto with a two-thirds vote in each chamber.

Appropriations Process

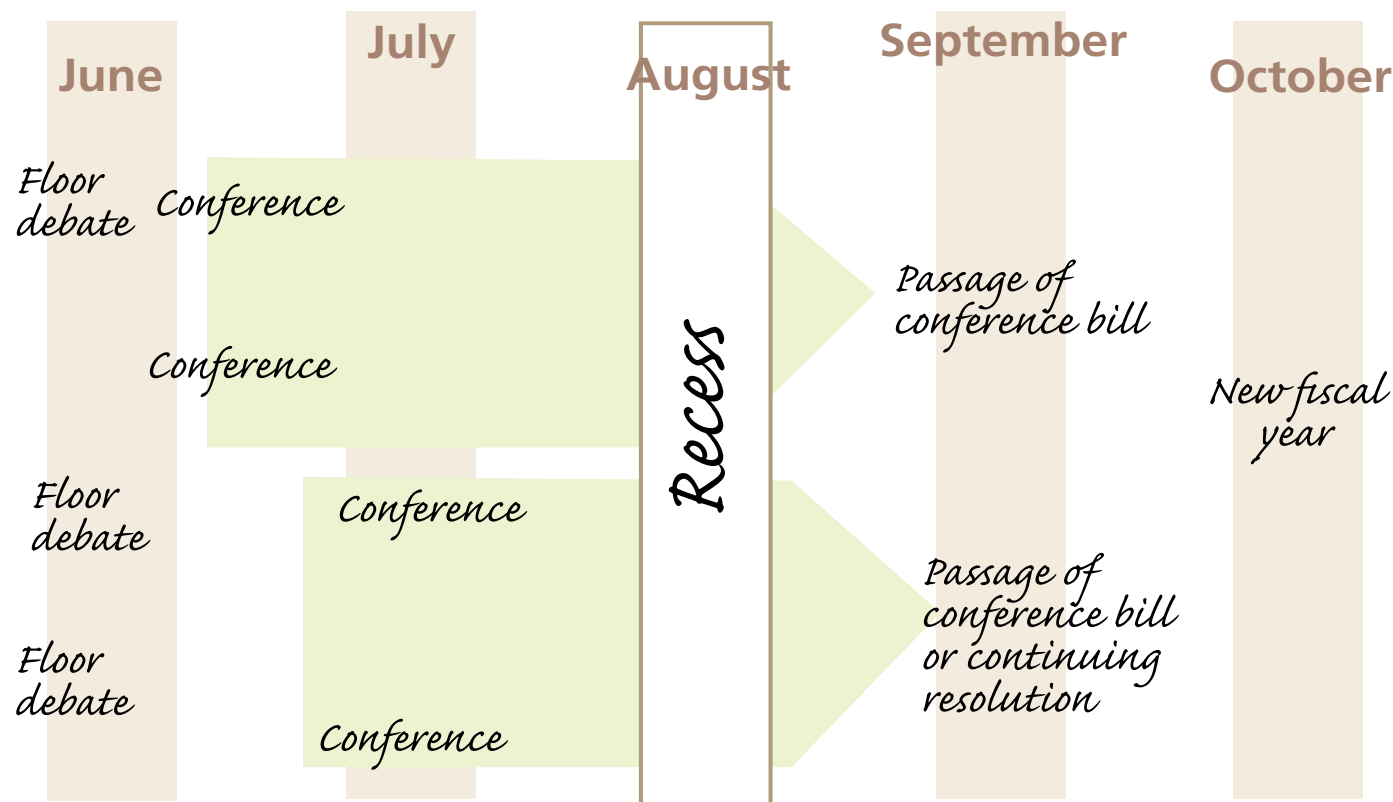
Unlike the DoD/DOE authorization bill, the 13 annual appropriations bills must be passed to ensure the smooth and continued operation of the federal government. For NNSA and its laboratories, the critical bill is the Energy and Water Development Appropriations bill. The House Energy and Water Subcommittee is chaired by Rep. Hobson (R-OH) and Rep. Visclosky (D-IN); its Senate counterpart is chaired by Sen. Domenici (R-NM) and Sen. Reid (D-NV).

The appropriations process follows the same basic path as the authorization process: hearings, markups at the subcommittee and full committee level, floor debate, bill passage, and conference bill. The notable difference is that the appropriations bill provides the actual dollars needed to execute a program. In late spring, each subcommittee receives a 302b allocation from the full committee. The 302b allocation is the actual dollars each subcommittee has to allocate for the programs under its jurisdiction. For the Nuclear

Weapons Program, this means competing with much more politically popular water projects.

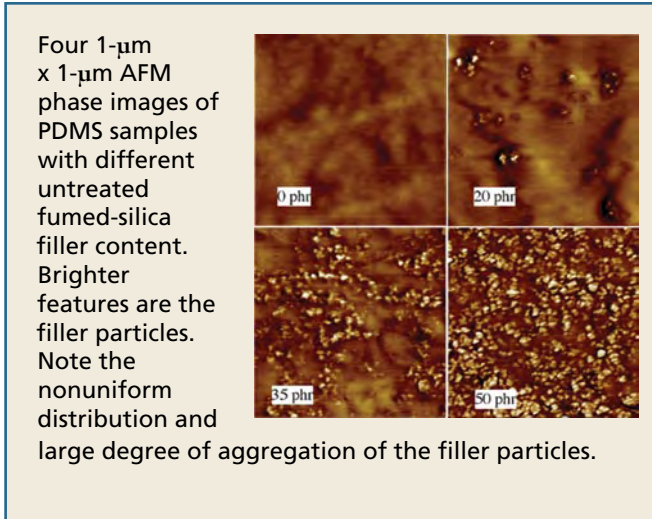
Over the last several years, the dynamics of the appropriations process has undergone significant change. Under the leadership of Rep. Hobson, the House Energy and Water Subcommittee is taking a much more proactive approach in a detailed review and analysis of the funding request and policy implications. In the FY05 House Energy and Water Development Bill, all funds for RNEP and Advanced Concepts were eliminated, but funding for dismantlement efforts at Pantex was increased by \$54M. The bill also directs DOE, beginning in FY06, to request direct funding for LDRD activities within each major appropriation. These funding and policy differences with the Senate Energy and Water Development Appropriations Subcommittee made completion of the bill very difficult. As a result, the FY05 Energy and Water Bill was folded into a larger omnibus appropriation measure that was signed by the President on December 8 in PL 108-477. [NWJ](#)

Jonathan Ventura, 606-0170, jonathan_v@lanl.gov
Dave Lyons, (202)488-5828, dcl Lyons@lanl.gov



Mechanical Properties, continued from page 27

Filler content and surface treatment clearly affected the mechanical properties of filled PDMS. For applications that require both high modulus and good elastic properties, the 35-phr untreated silica filler is optimum. This was demonstrated in tensile tests performed on dog-bone samples. Dog-bone samples from the same batches of four different filler content that were strained at two different rates, 0.1 mm/s and 10 mm/s, yielded the same results within experimental error.



With the exception of the 0-phr samples, which always broke, all samples made with untreated filler displayed a clear Mullins effect. Subsequent tensile tests showed the same Mullins stress-strain behavior rather than continuous softening. No Mullins effect was seen for the sample with HMDZ-treated filler: the mechanical properties were nearly linear and were significantly poorer than for the samples with untreated filler, even those with only 20-phr filler content.

Because the samples were made with the same polymer gum and had the same degree of cross-linking, we conclude that the interaction between polymer and filler was responsible for the observed change in mechanical properties from the untreated to treated filler samples. The stretched 35-phr samples heated overnight in an oven at 100°C and retested showed no recovery of prestretch mechanical behavior. Nor did the identical samples prestretched the same day, then retested one each at 1-week intervals, show any recovery of the original elastic properties. No change was seen for the sample stretched a third time. The 35-phr samples with fiduciary marks showed an average permanent set of about 3%.

Finally, the AFM phase images revealed a high degree of filler particle aggregation for all samples tested despite the extensive mixing procedure. The images also revealed a nonuniform distribution of the filler. The smallest particles observed were ≤ 20 nm in diameter—probably the individual filler particles.

Future AFM work will include in situ testing of samples to observe nanoscale deformation using filler particles as fiduciary marks. Work is in progress to measure mechanical properties as a function of angle to the initial stretch. [NWJ](#)

Point of contact:

Marilyn Hawley, 665-3600, hawley@lanl.gov

Acronyms Used in this Issue

BWXT	BWX Technoogies
DoD	US Department of Defense
DOE	US Department of Energy
DOE-LASO	DOE Los Alamos Site Office
EES	Earth and Environmental Sciences Division
FWO-UI	Facilities and Waste Operations Division, Utilities and Infrastructure Group
LANL	Los Alamos National Laboratory
LANSCE	Los Alamos Neutron Science Center
LLNL	Lawrence Livermore National Laboratory
NASA	National Aeronautics and Space Administration
NNSA	National Nuclear Security Administration
PX	BWXT Pantex Plant
SNL/NM	Sandia National Laboratories/New Mexico
TA	technical area
UC	University of California

A BACKWARD GLANCE

Edward Teller and the Navy

The success of Los Alamos and its scientists in creating the first atomic bombs brought acclaim, not only to J. Robert Oppenheimer, but to many of Project Y's senior scientists as well, including Edward Teller. In December 1945, the Navy asked Teller to comment on nuclear energy and national defense. In a wide-ranging response that included comments on missiles, radar, defense, and classification, Teller spent considerable effort describing possible changes to the Navy.

Teller stated that "...the overall effect of the atomic bomb will be to make the navy a much more important part of our national defense." Ships were mobile targets and therefore better able to escape atomic bombs. Ships also could serve as a defensive line thousands of miles from American shores and thus become an early warning system in case of missile attack.

However, Teller went on to state, "...the navy of the future will probably have to be rather different from

our present Navy." Teller noted that because armor provided little defense against an atomic bomb, the Navy could build lighter ships, an observation later demonstrated in the series of Operation Crossroads nuclear tests conducted in the Bikini Atoll lagoon in 1946. Teller also believed that big caliber guns would be replaced by rockets that would have little recoil, thereby further reducing the need for heavy ships.

Teller's most interesting comments concerned submarines. He suggested two possible designs. One design called for a small, power-producing pile (i.e., a nuclear reactor) with a shield to protect crews.

The shield, according to Teller, could be "...a big water tank, weighing at least 100 tons."

His second design proposed "...a power-producing pile with an attached engine and generator. This unit would propel itself and also have a cable leading to the submarine and [sic] providing the electromotor of the submarine with power." Although Teller noted the difficulties of this second proposal, it did have the advantage of being detachable and more easily repaired.

Teller's smaller, lighter Navy, he believed, would "...greatly add to the defense of our homeland against atomic bombs."

Teller championed research at Lawrence Radiation

Laboratory (now Lawrence Livermore National Laboratory) on the Navy's Polaris missile warhead, which was a great step forward in miniaturizing nuclear devices. In 1958, only a few months before nuclear testing was halted by an international nuclear test moratorium, an Operation Hardtack nuclear test validated the prototype design of the Polaris warhead. The Navy launched the first Polaris submarine armed with the new, lightweight nuclear weapon in 1960, far ahead of schedule. **NWJ**

Roger Meade, 667-3809, rzxm@lanl.gov

